

INVESTIGATION OF PRIMARY COSMIC RAYS ON THE
"PROTON-1" SPACECRAFTN. L. Grigorov, V. Ye. Nesterov, I. D. Rapoport,
I. A. Savenko and G. A. SkuridinTranslation of "Issledovaniye pervichnykh kosmicheskikh
luchey na nauchnoy stantsii 'Proton-I'"
Paper presented at 16th International Astronautical
Congress, Athens, September 1965

FACILITY FORM 802

N66-14060	
(ACCESSION NUMBER)	(THRU)
37	1
(PAGES)	(CODE)
	29
(NASA CR OR TMX OR AD NUMBER)	(CATEGORY)

GPO PRICE	\$	
CFSTI PRICE(S)	\$	
Hard copy (HC)		3.00
Microfiche (MF)		.50

653 July 65

NATIONAL AERONAUTICS AND SPACE ADMINISTRATION
WASHINGTON
DECEMBER 1965

CONTENTS

	Page
I. Chapter 1. The "Proton-1" Scientific Spacecraft	2
II. Chapter 2. Apparatus for Studying High- and Superhigh-Energy Particles and the Electron-Photon Components of Primary Cosmic Rays on the "Photon-1" Orbital Laboratory	7
III. Chapter 3. Preliminary Results of Cosmic Ray Study Conducted on the "Proton-1" Orbital Laboratory	48
IV. References	55

INVESTIGATION OF PRIMARY COSMIC RAYS ON THE
"PROTON-1" SPACECRAFTN. L. Grigorov, V. Ye. Nesterov, I. D. Rapoport,
I. A. Savenko and G. A. Skuridin

ABSTRACT

14060

The article is divided into chapters, each discussing a certain facet of studies on the "Proton-1" space laboratory. Chapter I examines the craft itself; Chapter II examines apparatus for studying high- and superhigh-energy particles and the electron-photon components of primary cosmic rays. Chapter III discusses preliminary results of cosmic ray study conducted on "Proton-1."

Handwritten signature

Chapter I. The "Proton-1" Scientific Spacecraft

13*

On 16 July 1965, using a new and powerful carrier rocket, the "Proton-1" scientific space laboratory was successfully inserted into a circumterrestrial orbit with an apogee of 627 km, a perigee of 120 km, and an orbital inclination of 63.6° (refs. 1 and 2).

The "Proton-1" space station is a complex, modern scientific laboratory (ref. 3). It is equipped with scientific apparatus, equipment for telemetric and extra-trajectory measurements, a system for indicating the attitude of the station in space, programatic devices, a power damping system, apparatus for remote radio control, and a temperature regulating system.

* Numbers given in margin indicate the pagination in the original foreign text.

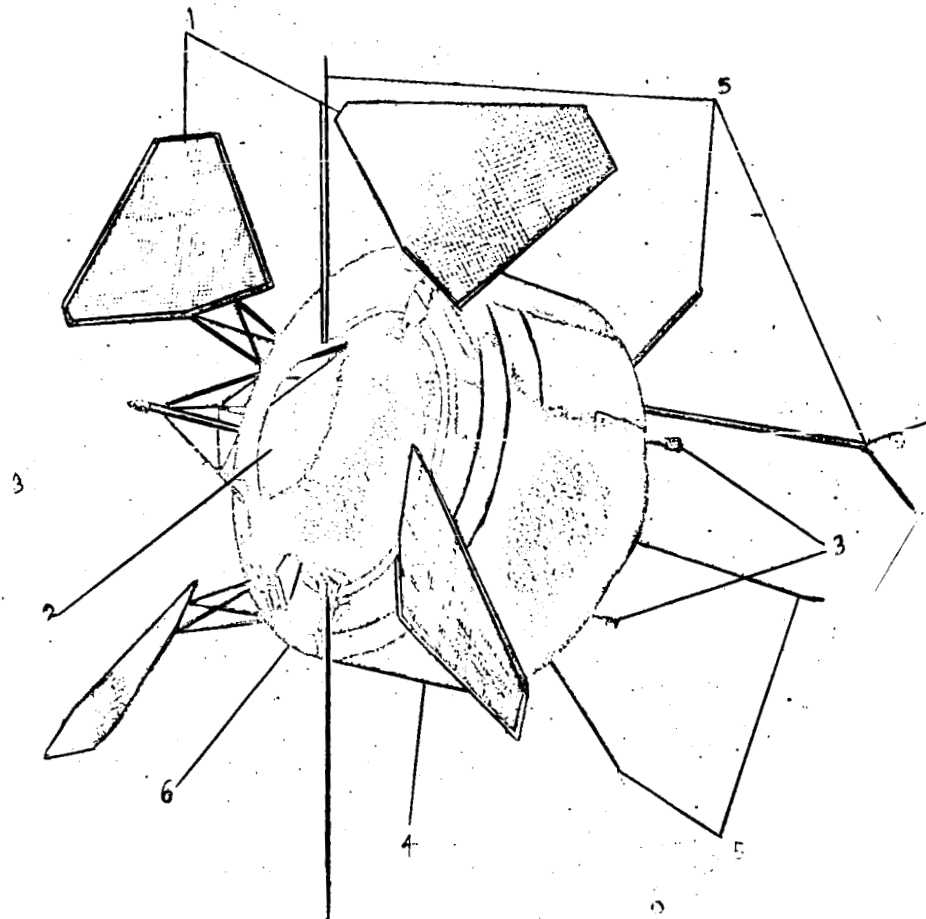


Figure 1. "Proton-1" Space Station. 1, Solar power plant panels; 2, hermetic hull; 3, vehicle attitude indicator system sensors; 4, outer envelope; 5, telemetry and radiocontrol system antennas and extra-trajectory measurement antennas; 6, chemical power source (batteries).

A general view of the "Proton-1" space station is shown in figure 1. Figure 2 shows the disposition of scientific and auxiliary equipment.

The inner hermetic hull of the station (2) provides protection against aerodynamic stresses and heat effects during insertion into orbit.

To prevent overheating and to cool the station during orbital flight, the hull of the station is insulated on the outside (4) with highly efficient thermal insulation.

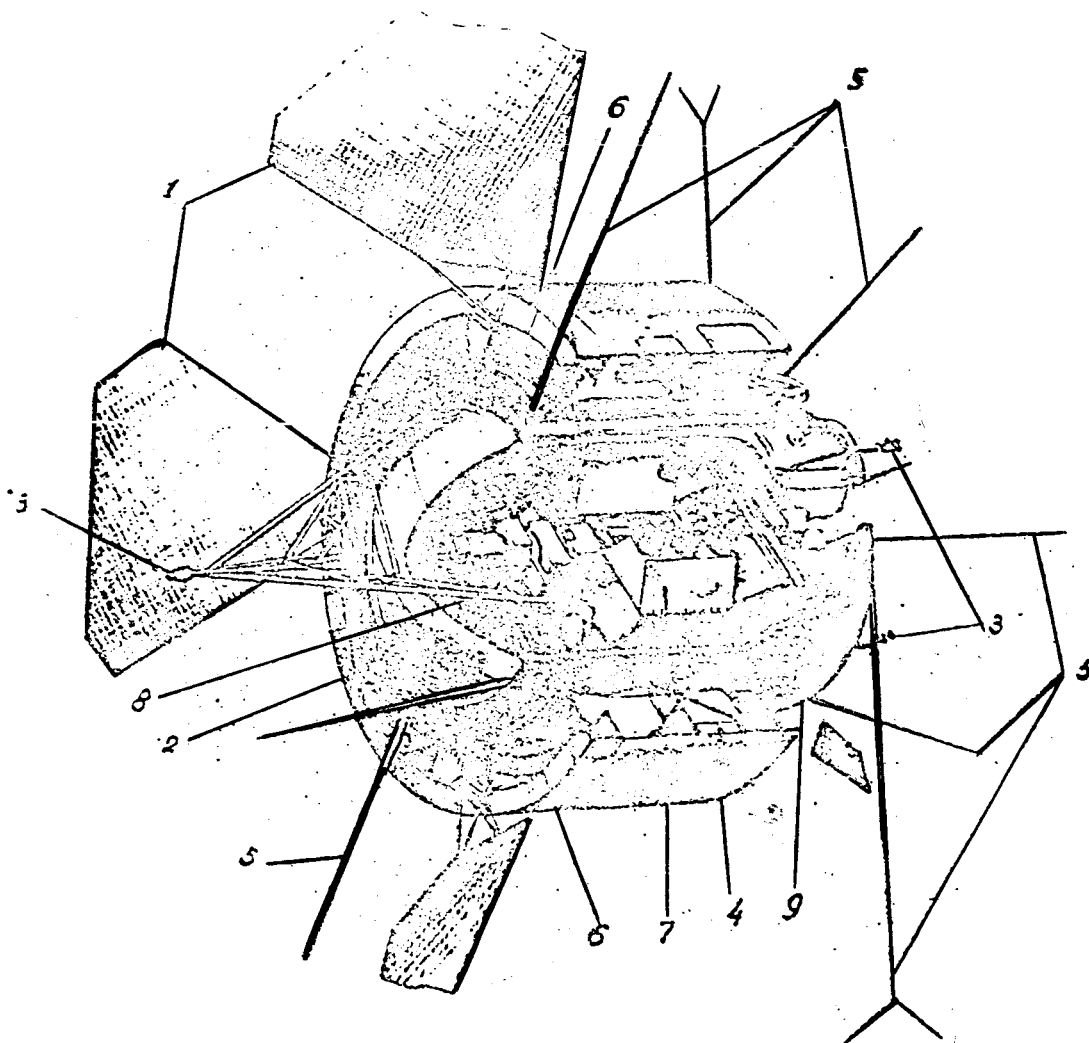


Figure 2. "Proton-1" Space Station, (Cutaway View). 1, Solar power plant panels; 2, hermetic hull; 3, vehicle attitude indicator; 4, outer envelope; 5, telemetry and radiocontrol system antennas and extra-trajectory measurement antennas; 6, chemical power source (batteries); 7, scientific equipment installation; 8, panels of on-board radioelectric equipment; 9, rejection heat exchanger.

Inside the hermetic hull, necessary temperature and normal pressure are maintained.

The hermetic hull of the space station (2) consists of a cylinder with a convex end. It houses scientific apparatus for studying cosmic rays (7), /4

an equipment system for indicating the position of the station in space (3), electrical and radio equipment, telemetry apparatus, and elements of the temperature regulating system.

On the outside of the hermetic hull are mounted solar battery panels (1) and shuttering mechanisms, and the sensors of the attitude indicator system (3). Elements of the electropneumatic power damping system are mounted on the stern. The heat rejection radiative heat exchanger is also located on the stern. The hull of the station also carries the antennas of the telemetry and radio control system and the system for extra-trajectory measurements (5).

Between the outer reinforced shell and the hull of the space station there are compartments for the chemical batteries and other equipment.

The complex aggregation of scientific equipment installed on the "Proton-1" required the solution of a serious problem, that of the transmission to Earth with a high degree of accuracy of all measured data. This is accomplished by the high-information capacity telemetry system installed on board the space station.

Reliable and accurate measurement of orbital parameters is accomplished by tracking stations on the ground and special radio signalling equipment carried on board.

The operation of the scientific apparatus and all systems of the station are controlled by automatic program devices and by radio control from Earth.

The indicator system makes it possible to determine the angular position of the station in space at every moment of time.

The damping system installed on board the station makes it possible to 15 stabilize the station after separation from the carrier rocket and to rotate it slowly around all three axes. Slow angular rotation of the station assures the normal operation of the solar batteries, a more even temperature regime, and an "unobstructed view" for the scientific apparatus.

The complex assortment of scientific equipment on board and the continuous operation of basic systems necessitated the creation and installation on board of a powerful solar power plant.

The solar batteries, grouped on special panels (1), furnish electrical power to the apparatus during the illuminated phase of the orbit and are also used to charge chemical storage batteries ("buffer" batteries) which supply power during the dark phase of the orbit, when the station is not illuminated by the sun.

The scientific equipment installed on board the "Proton-1" space laboratory for complex study of cosmic rays provides for:

- investigation of the energy spectrum and chemical composition of primary cosmic radiation particles with energies from 10^{10} to 10^{14} ev;
- measurement of the effective cross section of inelastic interaction of protons of various energies with other protons and with carbon nuclei;
- study of the electron component of primary cosmic radiation in the energy region from 3×10^8 to 2×10^{10} ev;
- measurement of galactic gamma-ray intensities and energy spectra in the energy range from 10^8 to 3×10^9 ev;
- study of solar cosmic rays and the radiation hazard which they present.

The equipment installed on board the "Proton-1" space station is functioning normally.

Introduction

It is known that the energy spectrum of primary cosmic radiation, which embraces about 10 orders of magnitude, is studied by direct measurement methods in a very narrow range of energies from 10^9 to 10^{10} ev. In the energy region $> 10^{10}$ ev the spectrum is reconstructed by indirect data: the μ -meson spectrum, measurement of electron-photon cascades by means of nuclear emulsions (at balloon altitudes) (ref. 4), and ionization chambers (at airplane altitudes) (ref. 5), while in the region of superhigh energies ($E \sim 10^{14}$ ev) information on the spectrum is obtained from extensive air showers (ref. 6).

All of these indirect methods of obtaining information on the spectrum of high- and superhigh-energy primary particles are based on certain a priori assumptions which are not always soundly enough founded on experiment or theory.

Besides this, the indirect methods used are completely unsuitable for studying the chemical composition of primary cosmic rays in the high- and superhigh-energy range. Even such a graphic method as the photoemulsion method cannot furnish a direct answer to the question of chemical composition at various particle energies, when the energies of the primary nuclei are determined by electromagnetic cascades generated by the primary cosmic ray particles in a relatively thin layer of matter.

The study of the energy spectrum and chemical composition in the energy range from 10^{11} to 10^{14} ev becomes particularly crucial in connection with investigations of various aspects of nuclear interactions of high- and superhigh-energy particles.

The application of methods more perfect than those used in earlier studies of ionization bursts at alpine altitudes and at sea level has shown that the integral spectrum of nuclear-active particles at alpine altitudes has an index $\gamma = 1.92 \pm 0.03$ (ref. 7). If the primary cosmic ray particle spectrum has an index γ of 1.67 to 1.7, it must be concluded that the absorption mean free path of nuclear-active particles depends on their energy.

Measurement of the flux of single nuclear-active particles with energies $\geq 2 \times 10^{12}$ ev, performed at alpine altitudes with an ionization calorimeter (ref. 8) showed a flux only one-tenth as great as that predicted from a primary proton spectrum with $\gamma = 1.7$, assuming the effective cross section of inelastic interactions between protons and light nuclei in the energy range 2×10^{10} to 2×10^{12} to remain strictly constant.

These examples show that a number of fundamental conclusions concerning the characteristics of the interaction of high-energy particles with atomic nuclei depend essentially on the type of energy spectrum and the composition of the primary particles in the region of high and superhigh energies.

For this reason it is extremely urgent (ref. 9) that direct measurements be made from large artificial Earth satellites of the energy spectrum and chemical composition of cosmic ray particles in the energy range from 10^{10} to 10^{14} ev, using exactly the same equipment for the whole range of primary particle energies (E) and charges (Z) measured.

The problems of the origin of cosmic rays are closely related to experimental studies of high-energy electrons and the study of gamma-quanta. /8

Experiments in this field are especially complex and because of the nature of the phenomena under study, the best place to conduct such experiments is in space.

For this reason an attempt was made to measure the flux and spectrum of electrons in the energy range from 3×10^8 to 10^{10} ev and the flux and spectrum of gamma-quanta in the energy range from 10^8 to 3×10^9 ev.

I. Apparatus

1) Instrumentation for studying high- and superhigh-energy particles (SEZ-14)

For investigating the energy spectrum and chemical composition of primary particles in the 10^{10} to 10^{14} -ev energy range, a special device, the SEZ-14 (spektrometr energii i zaryadov, "energy and charge spectrometer") was developed. This same instrument was also designed to measure effective cross sections of inelastic interaction between protons of various energies and other protons or hydrogen nuclei.

An overall view of the complex of scientific instruments for the study of cosmic rays is shown in figures 3 and 3a.

A schematic diagram of the SEZ-14 is given in figure 4. The SEZ-14 spectrometer consists of the following basic components:

- a) an energy detector designed to measure the energy E of each particle;
- b) polyethylene-graphite filters for measuring effective cross sections σ_{inel} of inelastic interactions between protons and other protons or hydrogen nuclei (4);
- c) proportional counters for measuring the charge Z of the primary particle (3);
- d) an interaction detector for registering cases of the interaction /9
of a primary proton of a given energy with the material of the filter;

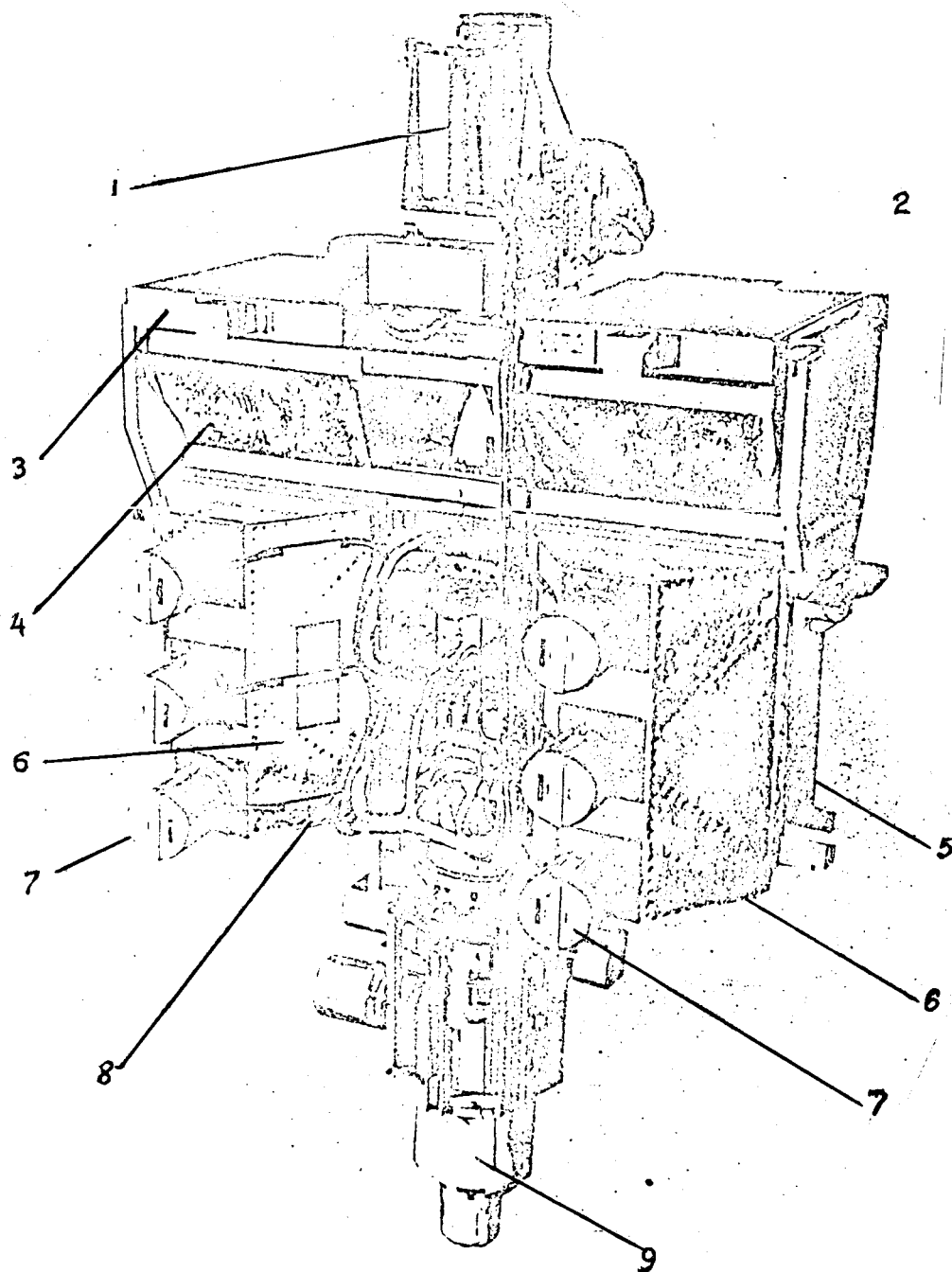


Figure 3. Cosmic Ray Study Instrumentation. 1, Spectrometer for cosmic ray particles of moderate energies; 2, gamma telescope; 3-8, ionization calorimeter complex; 9, high-energy electron recorder.

e) electronic components designed to pick up and record all relevant parameters.

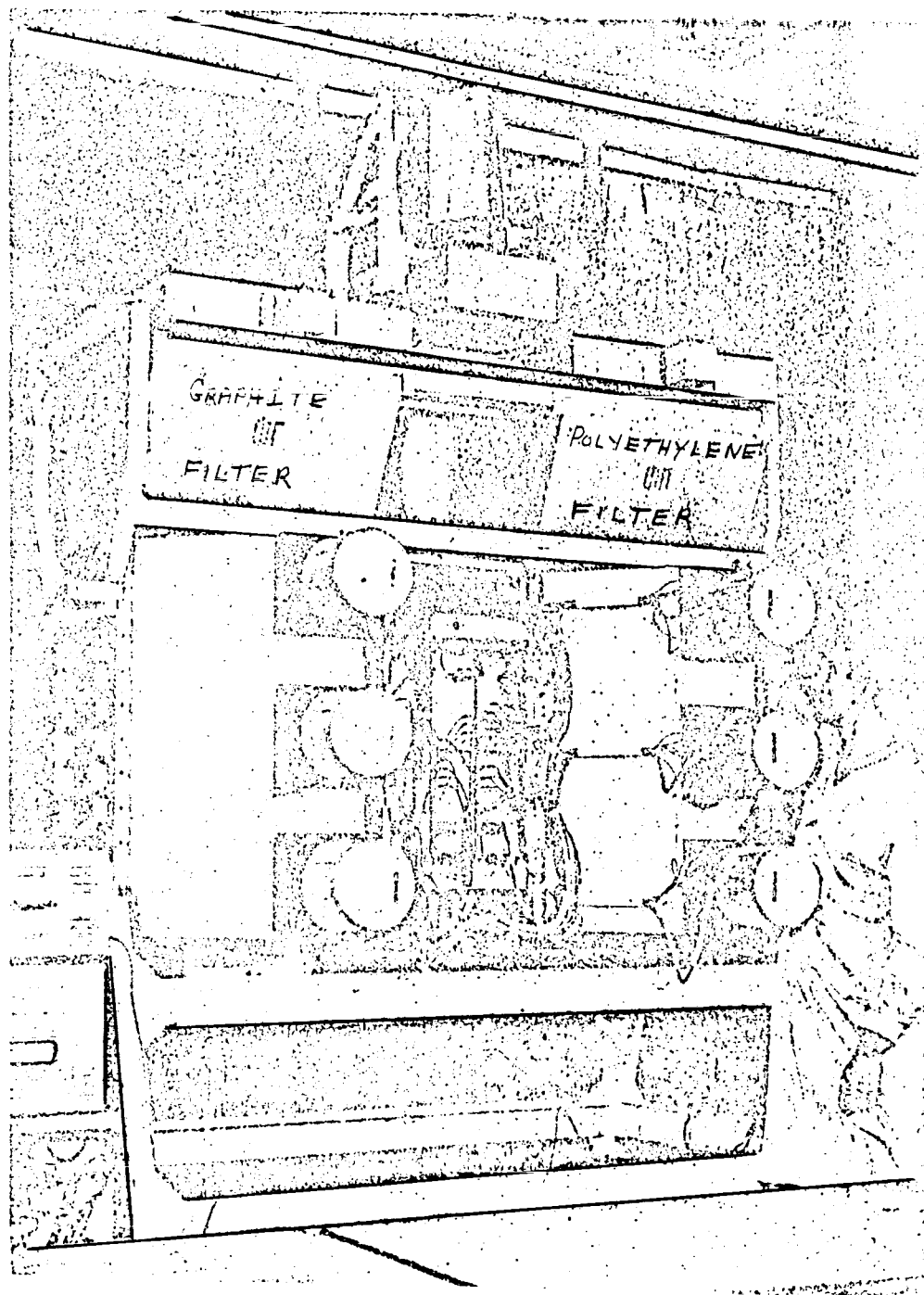


Figure 3a. General View of the SEZ (Energy-Charge Spectrometer) Complex.

The SEZ-14 apparatus was constructed as two independent identical units, each of which was a complete instrument capable of carrying out the whole program of measurements (determination of E , Z , and b_{inel}).

The filters (4) are mounted on an axis and can change position periodically during flight, so that one half the instrument is covered by the polyethylene filter and the other half by the graphite filter for a definite period of time, after which their positions are reversed; the new position is maintained for 12 hours, and then for a like period of time the filters are moved outside the solid angle of the installation. After that the cycle is repeated.

a. Energy Detector

The energy detector consists of a steel ionization calorimeter in which the ionization chambers have been replaced by plastic scintillators.

The ionization calorimeter consists of 9 steel plates each 5.5 cm thick and 10 layers of plastic scintillators between the steel plates and above and below the ionization calorimeter (fig. 1 /sic/, 1 to 10).

Each layer contains 12 plates of plastic scintillator measuring $5 \times 41 \text{ cm}^2$ /sic/ and 1.5 cm thick. These cover the whole cross sectional area of the ionization calorimeter. All surfaces of these plates are polished. For this reason light generated in the plate by the passage of a charged particle is fully reflected internally at the lateral edges of the plate and moves towards the /10 ends, and exits from the plate at the two ends.

All 10 layers of scintillators are enclosed on all sides of the ionization calorimeter by the diffuser-II (fig. 1), which consists of a rectangular pyramid having a photoelectric multiplier with a photocathode diameter of 15 cm at its apex. The inner surface of the diffuser and the edges of the steel plates are painted with a special white paint with a low light absorption.

The outputs of both photomultipliers (fig. 1 /sic/ , PEM-III and PEM-III^x) are connected together in such a way that the signals from each of them are

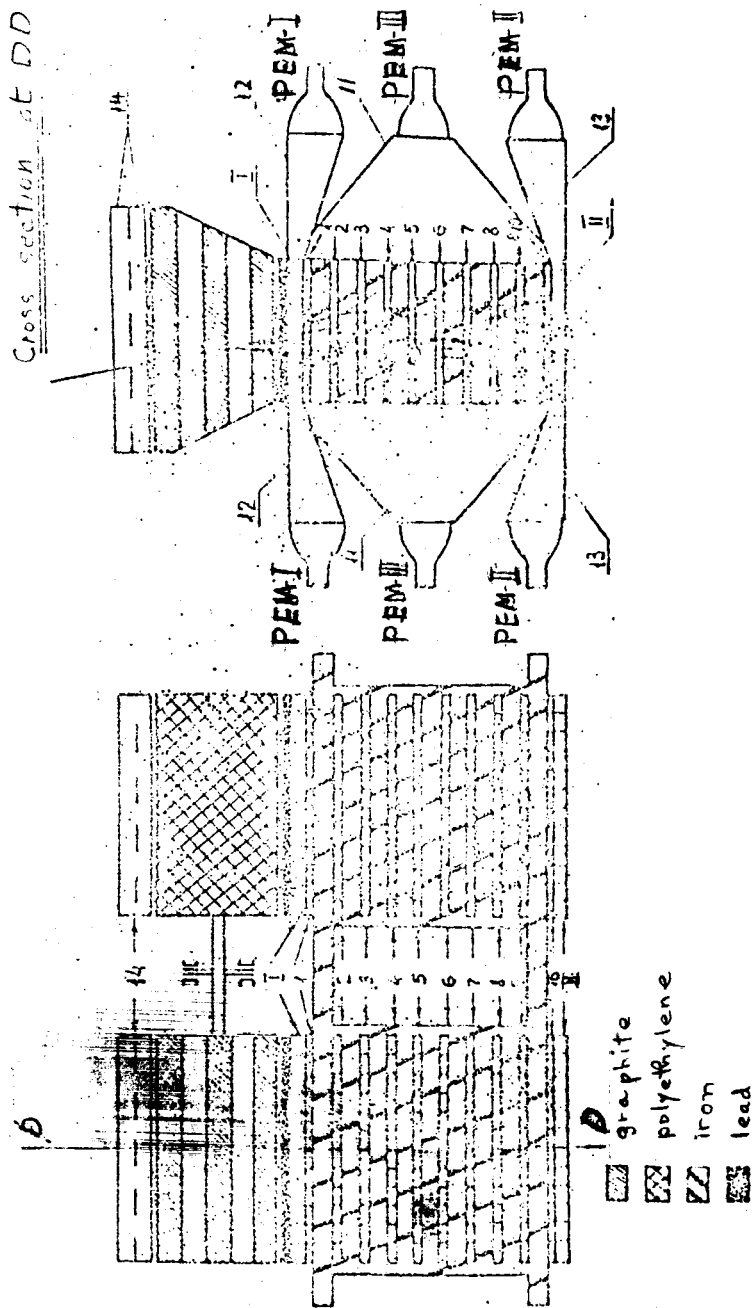


Figure 4. Schematic Diagram of the SEZ-14 Installation (in 2 Projections). 1-10, Plastic scintillator plates; 11, ionization calorimeter diffuser; I, interaction detector; 12, interaction detector diffuser; 13, scintillation counter; 14, proportional counters.

added. Thus, the input to the electronic circuit receives from these photomultipliers a signal whose amplitude is proportional to the total amount of light emitted through both end surfaces of the scintillating plastic plates.

The plastic scintillators used have a comparatively high absorption of the light of scintillation. Figure 5 (curve 1) gives the results of measurement of the amount of light (in proportional units) emitted through one end of the plate versus the distance from that end of the point traversed by the penetrating radiation (a collimating X-ray beam). The same figure (curve 2) shows the amount of light emitted from both ends of the plate. As can be seen from figure 2 /sic/, when the light is recorded by two photomultipliers, as it is in the SEZ-14, the maximum variance in the value of a light flash in proportion to the distance from the point of passage through the plate of the penetrating ray does not exceed 16 percent.

A check of light emission from the individual plates under identical /11 conditions of irradiation and light registration showed that the different plates had different light emission characteristics. Figure 6 displays the variation found in light emission values. (The light emission value "B" is determined with reference to the light emission of one plate which was taken as 100 percent.)

The plates in the ionization calorimeter were located at various distances and angles from the photomultiplier in the apex of the pyramid. Both these factors contributed to the circumstance that identical light flashes occurring in different plates would produce impulses of different amplitudes at the photomultiplier output. To eliminate this effect and render the amplitude of the photomultiplier output pulse independent of the location of the light flash in the ionization calorimeter, the ends of each scintillator plate were screened

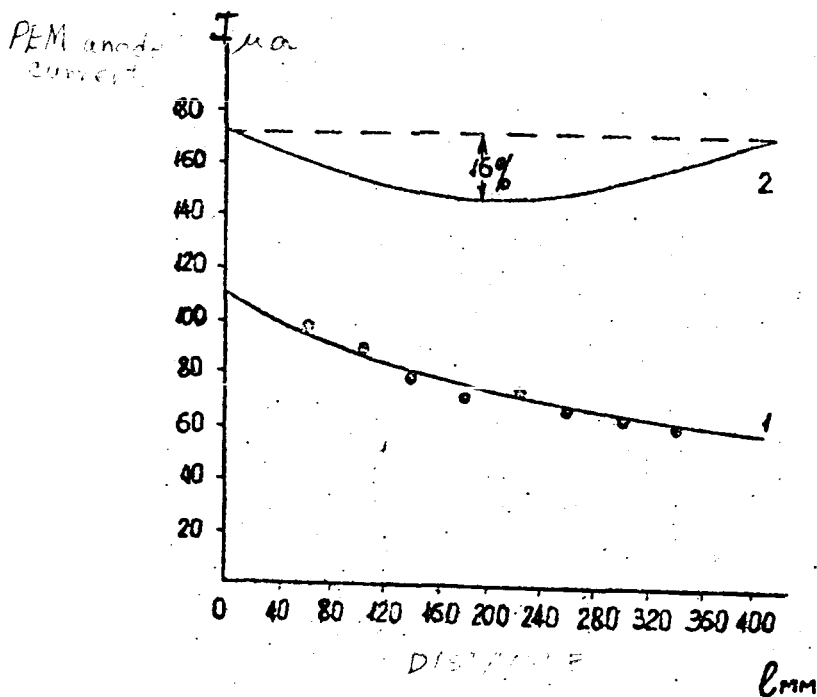


Figure 5. Dependence of Photomultiplier Anode Current (I) on the Distance l Between the End of the Plastic Scintillator Plate and the Site of Passage of Penetrating Radiation. 1, PEM receiving light from one end of plate; 2, PEM receiving light from both ends of plate.

with black paper. The width of the paper screen depended on the location of the plate in the ionization calorimeter and its relative light emission value .

By means of screens of appropriate width, all the plates were equalized in the amount of light reaching the photomultiplier when each of them was struck by a penetrating (X-ray) radiation of identical intensity.

This procedure reduced the variation in the light emission of the plates in the ionization calorimeter to ± 10 percent of the average light value recorded for a single plate.

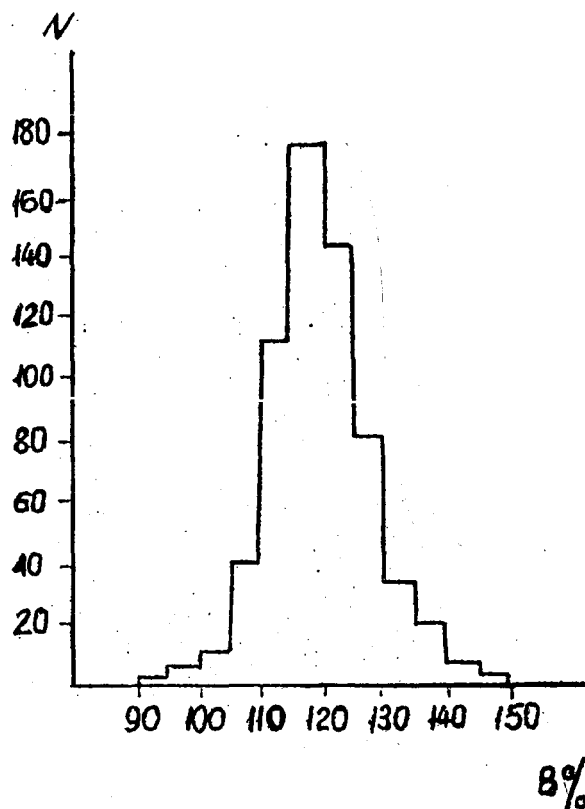


Figure 6. Distribution of Plastic Scintillator
Plates by Relative Light Emission Values B.

Figure 7 shows an experimental distribution of the light recorded from the different plates after[#]their equalization by means of screens, made for 4 ionization calorimeters. The average light value recorded for a single plate is taken as 100 percent.

To increase the amount of light reaching the photomultiplier from the /12 plates located at the extremes of the ionization calorimeter, the perimeter of the diffuser was bordered on the inside with an aluminum mirror strip 3 cm wide.

The degree of operational uniformity of the scintillator plates in the ionization calorimeter shows a wide amplitude distribution of pulses generated

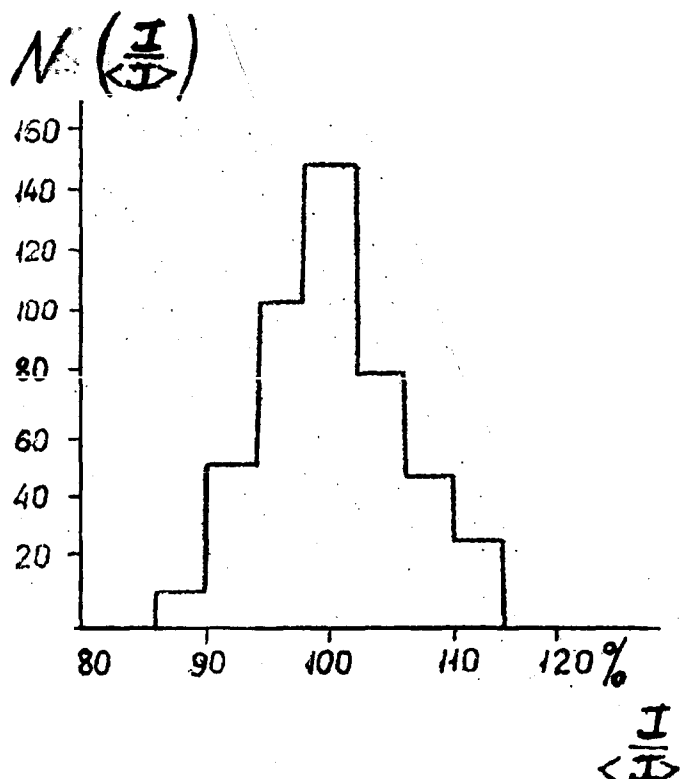


Figure 7. Distribution of Scintillator Plates of the Ionization Calorimeter by Relative Amounts of Light ($I/\langle I \rangle$) Reaching the PEM. $\langle I \rangle$ is the average amount of light reaching the PEM from one plate.

by the passage through the ionization calorimeter of cosmic ray mu-mesons.

Figure 8 shows this amplitude distribution, recorded by means of a 100-channel analyzer: "a" represents the first side of the SEZ-14, "b" represents the second side. Along the abscissa are the channel numbers, and along the ordinate, the number of cases with a given amplitude.

The energy E released in the ionization calorimeter is equal to

$$E = \lambda \int_0^{x_0} \gamma(x) dx \approx \lambda \sum_{i=1}^{10} \gamma_i$$

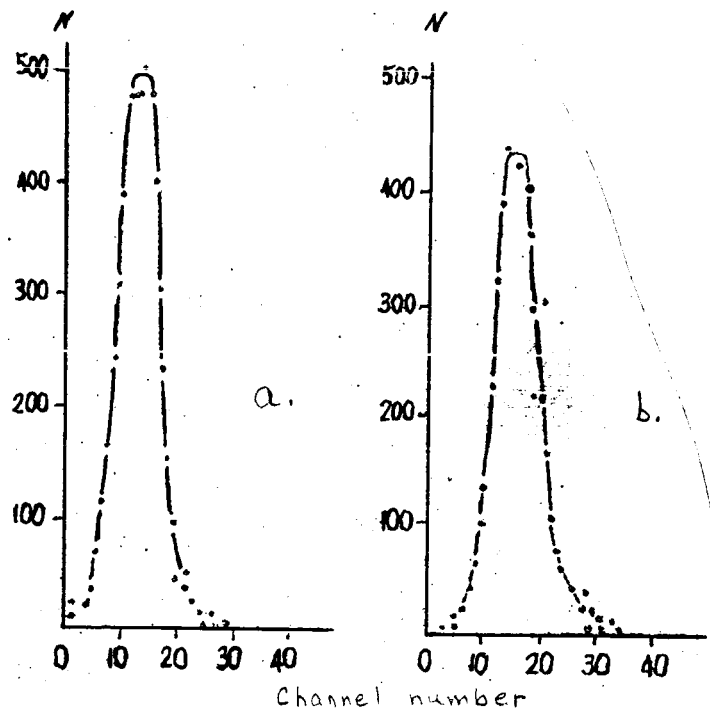


Figure 8. Amplitude Distribution of Pulses Generated in Ionization Calorimeter PEM by Passage of Cosmic Ray Mu-Mesons. Abscissa, amplitude analyzer channel numbers; Ordinate, number of cases with a given amplitude; a, for first side of SEZ-14; b, for second side.

If the light flash in the plastic scintillator were proportional to the energy lost through ionization by all particles in the plastic scintillator, then

$$E \sim \sum_{i=1}^{40} I_i \sim \sum_{i=1}^{40} S_i$$

where S_i is the intensity of the light flash produced in the i -th layer of scintillators.

However, for strongly ionizing particles there is no proportionality between I_i and S_i , so that the ionization calorimeter primarily detects the

energy given up by the primary particle over the whole thickness of the electron-photon component calorimeter.

The total thickness of the calorimeter (including the thickness of the plastic scintillators) $x_0 \approx 3$ nuclear mean free paths. In a layer of this thickness, the released energy E is in some cases less than the energy of /13 the primary particle E_0 . As a result, the measured flux $F_{\text{meas}} (\geq E)$ of particles with an energy $\geq E$ will not be equal to the actual flux $F_{\text{act}}(\geq E)$ of primary particles with an energy $\geq E$.

It is easy to show that for a power-law spectrum of the form $(F_{\text{act}} \geq E) = A/E^\gamma$, between F_{act} and F_{meas} will be found the ratio

$$F_{\text{act}}(\geq E) = B F_{\text{meas}}(\geq E), \quad (11)$$

where

$$\frac{1}{B} = \int_0^{x_0} U^\gamma(x) e^{-\frac{(x_0-x)}{L}} \frac{dx}{L}, \quad (21)$$

but

$$U^\gamma(x) = \int_0^1 U^\gamma(x) f(U, x) dU \quad (31)$$

Here (omission from original) represents the proportion of energy released in a calorimeter of thickness x , under the condition that the first interaction occurs at the edge of the ionization calorimeter, and $f(u, x)$ is the distribution function of the value $u(x)$ normalized so that

$$\int_0^1 f(u, x) dU = 1$$

L is the mean free path for an interaction of a primary particle with the matter of the ionization calorimeter.

Using the results obtained from the operation of an ionization calorimeter at the alpine station Aragats (ref. 8), it is possible to calculate $\overline{u^2(x)}$ and the coefficient "b", i.e., it is possible from the measured particle flux $F_{\text{meas}} (\geq E)$ to obtain the absolute flux of primary particles with an energy $\geq E - F_{\text{act}} (\geq E)$.

b. Interaction Detector (I)

The interaction detector (I in figure 1 /sic/) performs two functions:
 a) It registers the number of relativistic particles in a shower passing through it; and b) together with the lower scintillation counter (II in figure 1 /sic/) it is assigned a certain solid angle within the limits of which particles are registered.

Since we have set ourselves the goal of recording inelastic interactions beginning with protons with an energy of 10^{10} ev, whose inelastic interactions generate a small number of particles n , the interaction detector must be capable of detecting, with sufficient reliability, the passage through itself of single particles and showers with $n \geq 2$ relativistic particles. /14

In order to satisfy this requirement, the interaction detector is made up of bars of plastic scintillator material with a square cross section measuring $5 \times 5 \text{ cm}^2$ /sic/.

All faces of the bar are polished, so that light generated in any bar by the passage of a charged particle is subject to total internal reflection which directs it to the ends of the bar where it is emitted.

Opposite the ends of the bars on both sides of the interaction detector are diffusers (12 in figure 1 /sic/) with photoelectric multipliers (PEM-I and PEM-I^x) having a photocathode diameter of 15 cm mounted at their apices.

The interior surface of the diffusers is painted with special white pigment.

Both photomultipliers of the interaction detector are connected to a common load so that the output signal reaching the electronic component is proportional to the total amount of light registered by both photomultipliers.

By recording light from both ends of the bar, the dependence of the registered light flash amplitude on the location of the site of passage of the particles is weakened, as can be seen from figure 9.

In order to render the registered light flash independent of the position of the bar in the interaction detector (which contains 12 bars), a system of black paper screens making part of the cross section of the bar was used, as shown in figure 10. (The width of the screens was determined with reference to the light emission of each bar. The light emission of all bars was preliminarily measured with a collimated X-ray beam.) As a result (of these measures) the variation in light recorded from different bars does not exceed ± 10 percent from the average value. /15

Figure 11 shows the distribution of pulse amplitudes produced in the interaction detector by cosmic ray μ -mesons (sic) passing through the solid angle of the ionization calorimeter, which is bounded above by the interaction detector and below by the lower scintillation counter.

This distribution was obtained by means of a 100-channel amplitude analyzer.

The arrows^w in figure 11 indicate the threshold values of the amplitude discriminators 1 and 2 which distinguish the single particle region, the "window" between thresholds 1 and 2, from the region where the number of particles simultaneously passing through the interaction detector is equal to 2 or more ($n \geq 2$).

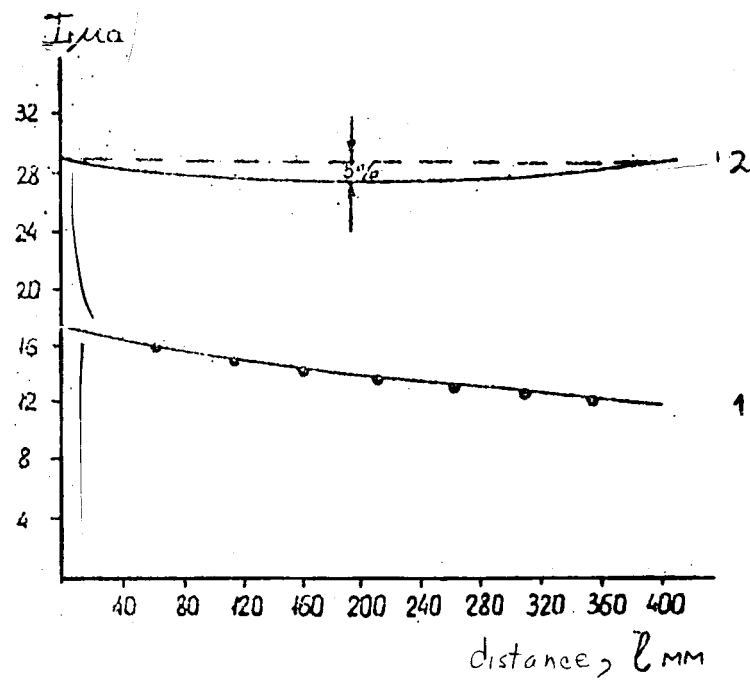


Figure 9. The same as figure 5, for plastic scintillator bars making up the interaction detector.

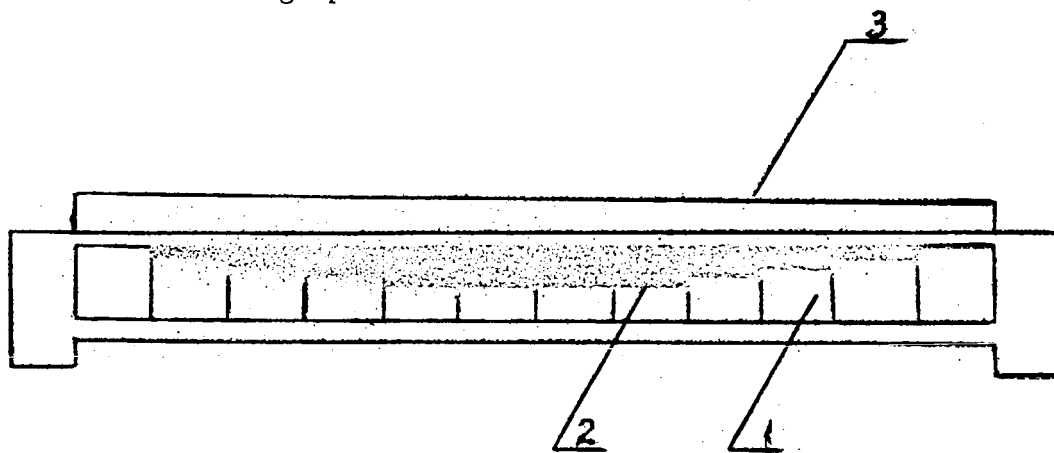


Figure 10. View of Interaction Detector from PEM. 1, Scintillating plastic bars; 2, black paper screens; 3, lead filter.

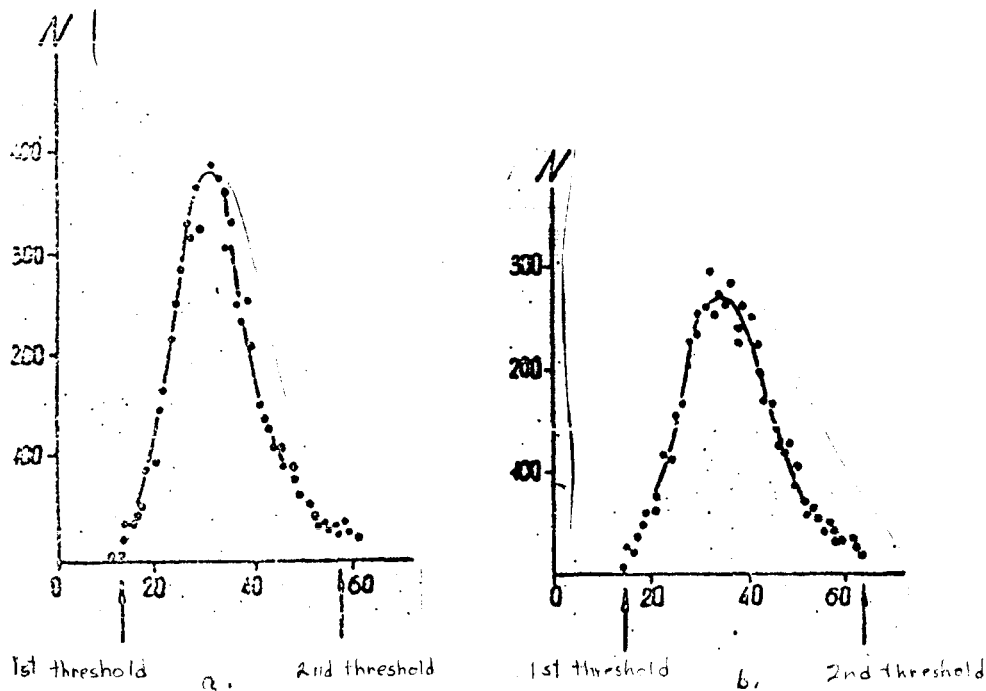


Figure 11. Amplitude Distribution of Pulses Generated in Interaction Detector PEM by Passage of Cosmic Ray mu-Mesons. Abscissa, amplitude analyzer channel numbers; ordinate, number of cases with a given amplitude; a, for first side of SEZ-14; b, for second side.

The values of the thresholds 1 and 2 are set such that: a) all relativistic particles passing through the interaction detector will be counted (position of threshold 1); and b) about 12 percent of all single particles will remain beyond the limits of threshold 2.

From figure 11 it is easily seen that there is a 14 percent probability that showers containing 2 relativistic particles will be registered as single relativistic particles. (Showers with $n = 3$ have a 100 percent probability of producing an impulse exceeding the value of threshold 2.)

To reduce the probability of miscounting interactions when the number of secondary charged particles $n = 2$, which is especially likely in the /16

primary proton energy range of 1 to 3×10^{10} ev, a layer of lead 2.5 cm thick is placed on top of the interaction detector. If neutral pi-mesons are formed by the interaction of a proton with nuclei of the filters, then even if the number of charged particles generated $n_s = 0$, the interaction will still be registered owing to the electron-photon shower which will be generated in the lead by the decay products of the neutral pi-mesons.

Estimates show that at primary proton energies $\sim 10^{10}$ ev, the probability that the interaction detector will miscount an interaction owing to the generation of a shower with $n = 2$ without any neutral pi-mesons amounts altogether to several percent.

Since altogether 3 nuclear mean free paths are contained within the SEZ-14 ionization calorimeter, the conditions of energy release in the calorimeter are different for particles undergoing interaction in the filter and particles which do not interact in the filter.

For this reason it is not possible to determine the effective cross section of inelastic interaction by comparing the number of particles with an energy E which interact in the filter with the total flux of particles with that energy (where E is the energy released in the ionization calorimeter), for the reason that such a comparison will yield an erroneous value for b^{inel} . In order to measure b^{inel} correctly it is necessary to sample the primary particles by their energy release in the calorimeter in such a way that this sampling will not change the conditions of energy release in the ionization calorimeter when filters are placed in the path of the particle.

This requirement can be satisfied by recording cases of the passage of particles through the filter without interaction.

In this case, if $N_0(E)dE$ represents the flux of protons striking the ionization calorimeter and releasing in it the energy E , $E + dE$, then the number of protons passing through the interaction detector without interacting in it (in the lead and plastic scintillator) and recorded as single particles (within 17 the "window") will equal

$$N_1(E)dE = N_0(E)dE K e^{-\frac{X_{pb}}{L_{pb}}} e^{-\frac{X_{n\lambda}}{L_{n\lambda}}} \quad (4.1)$$

where L_{pb} and $L_{n\lambda}$ are interaction mean free paths for protons in the lead and plastic scintillator, and X_{pb} and $X_{n\lambda}$ are thicknesses in g/cm^2 corresponding to the materials in the interaction detector. K is the fraction of relativistic particles with a single electrical charge striking the "window" (see fig. 11).

If a carbon filter with a thickness of X_c is placed in the path of the protons, then the number of protons releasing the energy E , $E + dE$ in the ionization counter and passing through this filter without interaction will be equal to

$$N_2(E)dE = N_0(E)dE K e^{-\frac{X_c}{L_c}} e^{-\frac{X_{pb}}{L_{pb}}} e^{-\frac{X_{n\lambda}}{L_{n\lambda}}} \quad (5.1)$$

Thus, having measured the intensity of single protons (without interaction) N_1 with no filter over the ionization calorimeter and N_2 with a graphite filter over the calorimeter, we obtain

$$e^{-\frac{X_c}{L_c}} = \frac{N_2(E)}{N_1(E)} \quad (6.1)$$

The ratio thus obtained will not be dependent on the exact value of the equipment parameters K and the energy E . It is only required of the apparatus that its parameters remain constant in time or change relatively slowly.

If a polyethylene filter containing the same amount of carbon as the graphite filter is placed over the ionization calorimeter, the number of protons releasing the energy E , $E + dE$ in ionization calorimeter which will pass through the filter without interacting in it and will be registered as single /18 particles, $N_3(E)dE$, will be equal to

$$N_3(E)dE = N_n(E)dE \cdot K \cdot e^{-\frac{X_H}{L_H}} \cdot e^{-\frac{X_C}{L_C}} \cdot e^{-\frac{X_{Pb}}{L_{Pb}}} \cdot e^{-\frac{X_{Al}}{L_{Al}}} \quad (7.1)$$

and

$$e^{-\frac{X_H}{L_H}} = \frac{N_3(E)}{N_2(E)} \quad (8.1)$$

In the expressions 5.1, 6.1, 7.1, and 8.1, L_C and L_H represent the mean free paths for inelastic interaction of protons in carbon and hydrogen, respectively.

The lower scintillation counter is similar in construction to the interaction detector, differing from it only by the absence of the lead filter.

c. Proportional Counters

For determining the charge of the primary particle, 2 proportional counters are mounted above each ionization calorimeter (14 in figure 4).

Both counters are mounted in a single hermetic aluminum housing having the form of a flat parallelepiped. Each counter consists of 6 sections measuring 10 x 5 cm. Along each section is stretched a wolframite filament 0.1 mm in diameter and 70 cm long. The filaments of all 6 sections are joined inside the housing and the common output is led outside through an insulator. (A transverse cross section of the counter is shown in figure 12.)

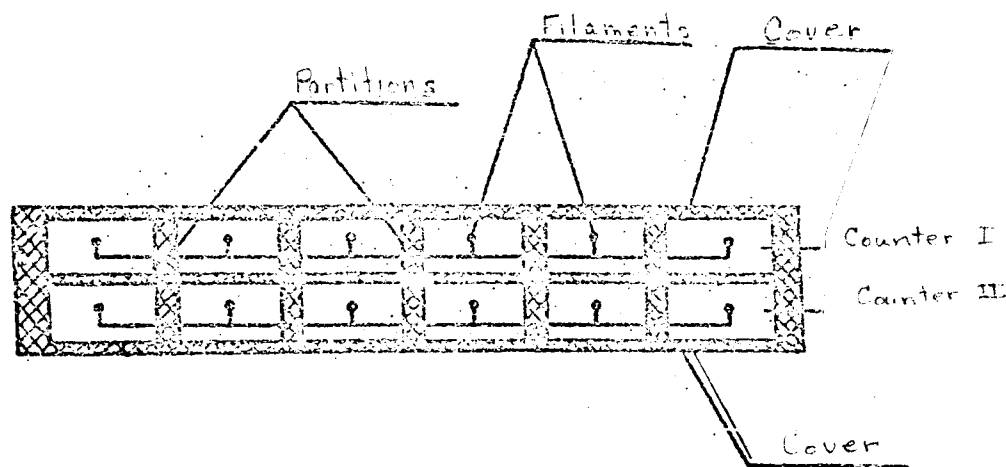


Figure 12. Schematic Cross Section of Proportional Counters in Their Container (Perpendicular to filaments).

The covers of the counter are 2.5 mm thick. The partition separating the first counter from the 2nd is also of aluminum and is 2 mm thick.

The chambers of the 2 counters communicate through special apertures provided to assure identical gas composition and pressure in both counters. The counters are filled with argon + 10 percent methane at a total pressure of 300 mm Hg. Both counters receive an identical stabilized voltage of 1750 V through individual resistances. Under these conditions the output /19 pulse generated by the passage of a single relativistic particle through the counter is equal to 720 μV .

A test showed that the gas multiplication in all chambers of both counters was identical to within ± 10 percent.

The distribution of amplitudes of pulses generated by cosmic ray mu-mesons passing through the proportional counters mounted in the SEZ-14 apparatus is shown in figure 13.

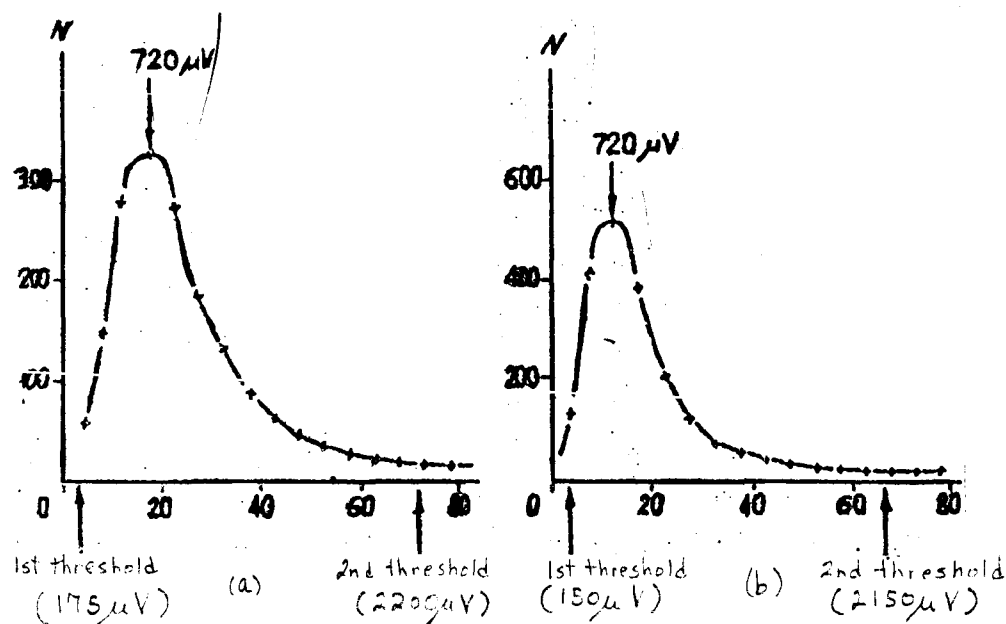


Figure 13. Example of Amplitude Distribution of Pulses Generated by Cosmic Ray mu-Mesons in the Proportional Counters. a, in first counter; b, in second counter; abscissa, amplitude analyzer channel number; ordinate, number of cases with a given amplitude.

The slightly different position of the distribution maximums in counters I and II is due to differences in the amplification coefficients of the amplifiers connected to each counter.

The arrows over the curves show the position of the channel into which a $720 \mu V$ pulse falls.

From figure 13 it can be seen that both counters have practically identical gas multiplication at an identical voltage of 1750 V.

Singly-charged relativistic particles are registered in the SEZ-14 in those cases when the proportional counter pulses accompanying them are within the "window" demarcated by the 1st and 2d thresholds (whose values are given in

figure 13). For the chosen values of the 2d threshold about 10 percent of the singly-charged particles are outside the "window." Since the pulses in both counters must be within the "window" limits for a singly-charged particle to be registered, the registration efficiency of the two proportional counters for singly-charged particles amounts to 80 percent. The probability of a proton imitating an alpha-particle (simultaneous generation in both counters of pulses lying beyond the 2d threshold) is about 1 percent. The probability of a relativistic alpha-particle generating a pulse lying within the "window" in 1/20 one of the counters is about 10 percent. Therefore, the probability of registering an alpha-particle as a proton (with the pulse from the alpha-particle lying within the "window" in both counters) is about 1 percent.

It should be noted that an admixture of alpha-particles in the flux of particles registered as singly-charged has no essential effect on the measurement of the effective cross section of inelastic interaction, since such particles will always produce a pulse lying beyond the 2d threshold in the interaction detector, i.e., beyond the limits of the "window" for single, singly-charged particles.

d. Filters

The polyethylene and graphite are placed in light-weight, duraluminum containers. The thickness of the polyethylene filter is about 35 g/cm^2 . The thickness of the graphite filter is about 30 g/cm^2 . Since the density of the graphite is greater than that of the polyethylene, geometric uniformity of the two filters was achieved by making the carbon filter in three layers of different thicknesses placed at three levels: on the bottom of the container, in the center of the container, and under the top cover of the container.

Geometrical uniformity of the two filters is important only in the measurement of the effective cross sections of inelastic interactions of particles of relatively low energies (to 3×10^{10} ev), since at such energies the angle of scattering of the secondary particles is still quite large.

The filters in their housings are mounted on an axis and can be automatically rotated to change their positions with relation to the two SEZ-14 ionization calorimeters. Filter position is changed on command from Earth and is radioed to Earth along with all other information.

e. Operating Principles of the SEZ-14 Instrument

/21

We will consider the operation of one side of the SEZ-14.

Accomplishment of the program of measurements--of the energy spectrum and chemical composition of primary particles of various energies and of the energy imparted to neutral pi-mesons by protons of various energies interacting with the matter in the filter--requires that multidimensional amplitude analysis be performed in the SEZ-14 instrument.

This is done in the following manner:

The pulses from each detector are fed into a system of integral and differential-type amplitude discriminators.

Specifically, the pulses from the ionization calorimeter are fed into 9 integral-type discriminators which divide the entire range of energy releases in the ionization calorimeter from 10^{10} to 10^{14} ev into 8 equivalent (on a logarithmic scale) intervals.

Let us arbitrarily assign each discriminator an index E_i ($i = 1$ to 9). If both scintillation counters (I and II) are actuated simultaneously during the operation of the discriminator E_i , that is, if a particle has passed

through the solid angle of the ionization calorimeter, a supplementary signal, which we will designate E_{Si} , will be generated.

Pulses from the interaction detector act upon the differential discriminator, which generates pulses limited by the 1st and 2d thresholds (see figure 2). This discriminator detects cases of the passage through the interaction detector of a single singly-charged particle. ("Particle" is to be understood as "relativistic particle" throughout.) We will designate the operation of this discriminator with the index N_1 .

If a pulse from the interaction detector exceeds the 2d threshold, /22 it actuates the integral discriminator N_K , where $K = 2$ to 9. The K indices correspond to the following numbers of particles in a shower passing through the interaction detector (see table 1).

Pulses from each proportional counter actuate the differential discriminators detecting different groups of nuclei. We will designate the functioning of the j -th discriminator by Z'_j , Z''_j (with ' or '' depending on whether proportional counter I or II is meant) where $j = 1$ to 8.

Z'_1 and Z''_1 correspond to a particle with a charge of 1, i.e., a pulse from the counter lying within the limits of the "window" formed by the 1st and 2d thresholds;

Z'_2 and Z''_2 , to the "window" distinguishing alpha-particles;

TABLE 1

K	2	3	4	5	6	7	8	9
$n \geq 2 \geq 50 \geq 200 \geq 500 \geq 10^3 \geq 3 \cdot 10^3 \geq 10^4 \geq 3 \cdot 10^4$ particles								

Translator's note: Original " \geq " should be " \leq ".

Z'_3 and Z''_3 , to the "window" distinguishing the nucleus group Li, Be and B;

Z'_4 and Z''_4 , to the "window" distinguishing the nucleus group C, N, O, and further groups of heavier nuclei.

If discriminators with the same j -number function simultaneously (within the limits of a resolution time equal to 6 μ sec) in both proportional counter channels, a signal Z_j is formed indicating that in both counters the pulse generated by the passage of a particle corresponds to the same charge interval.

Further on, these signals-- E_{S_j} , N_K , and Z_j (we will call them "elementary")--are fed into differential binary and ternary coincidence circuits which register various combinations of "elementary" signals. /23

Combinations of the type Z_j , E_{S_i} yield the integral energy spectrum of particles with charges in the group Z_j ($j = 2$ to 8). For protons Z_1 ($j = 1$) there is a special measurement routine.

Coincidences of the type Z , N_K (where $K \geq 2$) give the spectrum of "ionization beams" generated by protons in the filters.

Ternary combinations of the signals Z_1 , N_1 , E_{S_j} ($i = 1$ to 9) give the flux of protons with energies $\geq E_i$ traversing the solid angle of the apparatus and passing through the filter without interaction.

Coincidences of the elementary signals Z_1 , N_2 , E_{S_i} give the flux of protons of various energies traversing the solid angle of the apparatus and interacting in the filters.

Because of the rather high luminosity of each side of the SEZ-14 apparatus, the number of energy release events in the ionization calorimeter with $E_{S_i} \leq E_{S_s}$ ($E_{S_s} \approx 10^{12}$ ev) is too great to permit individual analysis of all parameters

of an individual particle. Therefore for E_i ($i = 1$ to 5), the various combinations of "elementary" signal coincidences are counted and stored in the "memory" system, which is interrogated during communications transmission sessions between the AES and Earth.

Events corresponding to particles with an energy $\geq E_{S_s}$ are fairly infrequent, so that it is possible to record the values of Z' , Z'' , and Z_0 and the value of N_K individually for each particle with E_{S_i} ($i \geq 5$), and to identify these events during later processing of the recorded data on the ground.

With this method, the recorded results can be used to verify the proper functioning of the apparatus: electronic circuits for comparing the Z'_i and Z''_i signals and processing the Z_i signal, electronic circuits for processing the E_{S_i} signal (at least for $i \geq 6$), the invariance of the sensitivity of /24 the interaction detector, and the stability of a number of other parameters.

To furnish a comparison of the statistical and individual methods of sampling and registering events, cases with an energy E_{S_s} were recorded by both methods.

To study the types of energy spectrum in the superhigh-energy particle region, information was gathered separately on the number of particles of various energies striking the ionization calorimeter from all directions E_i ($i = 1$ to 9).

2) Instrumentation for Recording High-Energy Primary Electrons (SEZ-12)

The basic obstacle to the study of the electron component of cosmic radiation is that the electron flux is quite small, on the order of 1 percent of the proton flux. For this reason, apparatus designed for the registration of electrons must exclude the possibility of imitation of electrons by protons. If this possibility cannot be wholly eliminated, then the experimental study

of electrons must at least be arranged so that cases of imitation, which we will call instrument noise, can be individually identified.

If measurements are made of primary cosmic ray electrons with equipment installed on an AES, it becomes possible to use the geomagnetic effects of cosmic rays to determine instrument noise from the direct results of the measurements and to identify the electron component more reliably.

When AES measurement capabilities include the unambiguous identification of electrons, it becomes possible to determine the charge composition (positron --electron ratio) of the electron component in the electron energy region $\sim 10^{10}$ ev based on measurement of East-West asymmetry in the intensity of the /25 electron component.

The instrument designed for studying the electron component of cosmic rays, the SEZ-12 (electron spectrometer), is diagrammed schematically in figure 14.

It consists of the following basic elements:

- 1) A telescope made up of 2 scintillation counters (1 and 2);
 - 2) A gas-filled Cerenkov counter (3);
 - 3) An electron energy detector (7) with a thick absorption filter (5);
- and
- 4) A shower detector (8).

a. Construction and Nomenclature of the Basic Elements of the SEZ-12 Instrument

1. The scintillators for the telescope are made of a scintillating plastic and have the form of cylinders 13.6 cm in diameter and 1.5 cm high.

Scintillator (1) faces the photomultiplier PEM-1, and scintillator (2) faces PEM-2 (see figure 14).

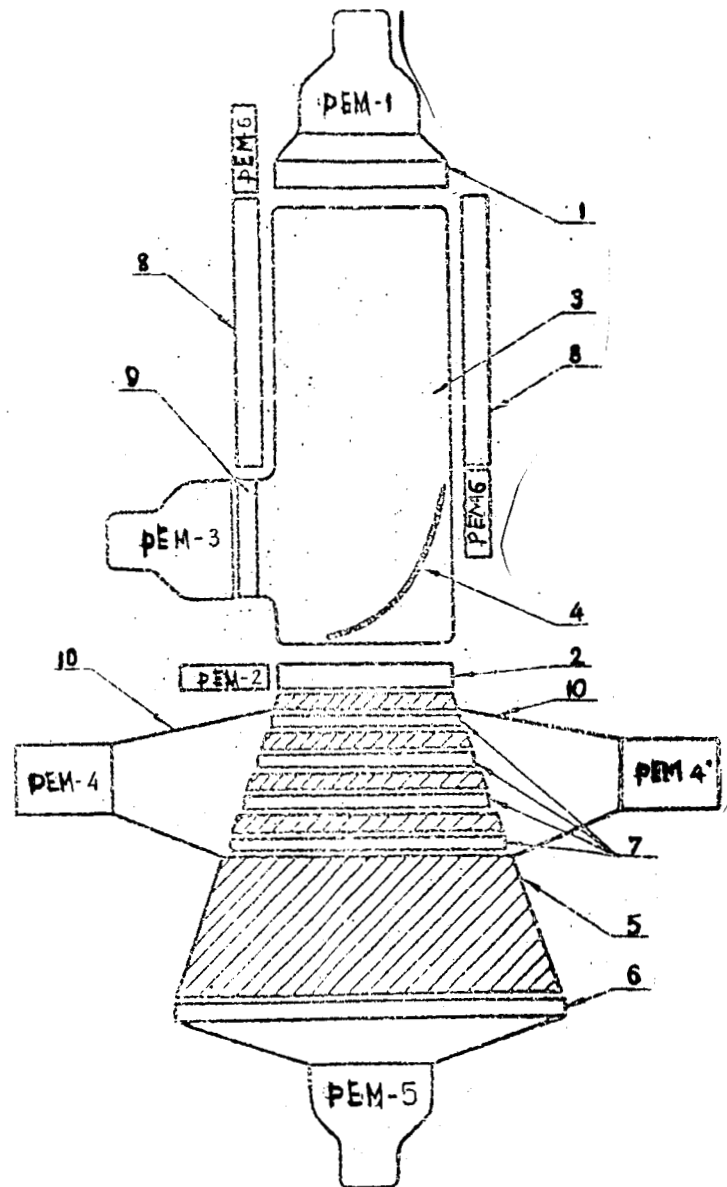


Figure 14. Schematic Diagram of the SEZ-12 Instrument. 1, (with PEM-1) scintillation counter; 2, (with PEM-2) scintillation counter; 3, gas-filled Cerenkov counter (with PEM-3); 4, parabolic mirror; 5, lead filter; 6, (with PEM-5) scintillation counter; 7, energy detector scintillators; 8, scintillating plastic cylinder; 9, plexiglass window; 10, energy detector diffusers.

The counters of the telescope fulfill two functions: they define the solid angle within whose limits charged particles will be registered. (The geometric factor of this telescope is equal to $5.0 \text{ cm}^2 \text{ ster.}$)

In addition, the PEM-1 photomultiplier is connected to a differential amplitude analyzer which selects only those particles with a charge $Z = 1$. By this means it is possible to exclude multicharged primary cosmic ray particles as well as instances of high-energy proton interaction in the scintillator itself or in the PEM-1 mounted above the scintillator.

2. The gas-filled Cerenkov counter consists of an aluminum-alloy /26
cylinder 53 cm high and 20 cm in diameter. The thickness of both the upper and lower surfaces is 0.4 cm. On the side of the counter, outside the limits of the solid angle defined by counters (1) and (2), the cylinder has a plexiglass window (9). The counter is filled with freon-13 at a pressure of 11 atm.

Cerenkov radiation generated in the counter by particles traversing the limits of the solid angle of the instrument is reflected by a parabolic mirror (4) into the photomultiplier PEM-3.

The gas-filled Cerenkov counter fulfills two functions:

Firstly, it records only those particles which have an energy not lower than E_{\min} , where $E_{\min} \approx 7 m_0 c^2$ (m_0 is the rest mass of the particle). (The effective registration threshold $E_{\text{thr}} \sim 10 m_0 c^2$.) That is to say that protons can be registered by the Cerenkov counter if their energy $\geq 10^{10} \text{ ev}$.

The lower limit of electron energies registered by the instrument is basically limited not by the Cerenkov counter, but by the thickness of the matter they must pass through in order to satisfy the requirements for the registration of events.

Secondly, the Cerenkov counter registers only those particles which enter the instrument through counter (1) in figure 14 (moving from top to bottom), and does not register those moving in the opposite direction (from bottom to top).

3. The energy detector consists of 4 lead plates each 1 cm thick. Between the lead plates are plastic scintillators, also each 1 cm thick. Specially chosen screens cover the end parts of the scintillators, ensuring that an identical quantity of light reaches the photomultiplier from each plate when it is traversed by penetrating radiation (collimated X-rays) of even intensity. Because of these screens, the amount of light emitted by the plate is independent of the site of passage of a charged particle through the plate over 80 percent of its area. /27

The amplitude distribution of light flashes generated in the energy detector by cosmic ray mu-mesons traversing the boundaries of the solid angle of the telescope is shown in figure 15.

Light from the scintillators is emitted through the ends and falls partly on the photomultipliers PEM-4 and PEM-4^x, and partly on the walls of the diffuser (10), the interior of which is covered with a white paint having a low coefficient of absorption.

The outputs of both PEM-4 photomultipliers are connected together so that the total signal is proportional to the amount of light reaching both photomultipliers.

Two photomultipliers are used in order to eliminate dependence of signal amplitude on the site of passage of a particle through the plastic scintillators of the energy detector.

The total thickness of the lead plates in the energy detector is such that for electron energies $\leq 10^{10}$ ev, a proportionality exists between the

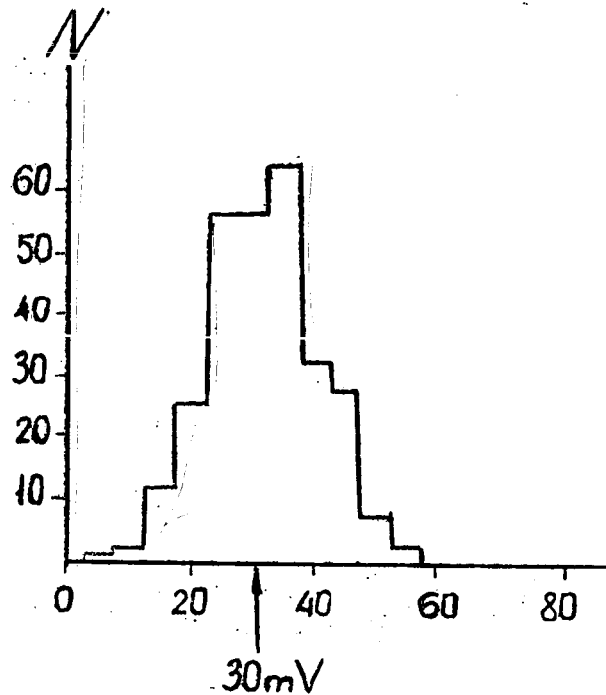


Figure 15. Amplitude Distribution of Pulses Generated in the SEZ-12 by Cosmic Ray mu-Mesons. Ab_X^S , amplitude analyzer channel number; ordinate, number of cases with a given amplitude; 30 mV, amplitude of PEM output signal corresponding to the most probable pulse amplitude.

energy of the electron E_e and $\int_0^{t_0} N(t, E_e) dt$, where $N(t, E_e)$ is the number at a depth of t shower units in an electromagnetic shower generated by electrons with an energy of E_e ($t \approx 7$ shower units).

Since the amplitude of a light flash in the energy detector is $S \sim \int_0^t N(t, E_e) dt$ then $E_e \sim S$.

Beneath the energy detector is a heavy lead filter (5), 12 cm thick, which covers the solid angle of the telescope. Under this filter is a

/28

scintillation counter (6) with a photomultiplier PEM-5. This counter serves to determine the penetration capacity of the particles registered by the instrument.

4. The shower detector (8) consists of a cylinder made of scintillating plastic surrounding the gas-filled Cerenkov counter. It is monitored by 4 photomultipliers (PEM-6) connected in parallel (figure 6 /sic/ shows only 2 of these PEM-6 photomultipliers). The purpose of the shower detector is to significantly reduce the probability of the registration of secondary particles (mainly pi-mesons) which might be generated by high-energy protons either in the walls of the gas-filled Cerenkov counter or in the material of the AES located over the SEZ-12 instrument. (Within the limits of the solid angle of the instrument the average thickness of matter located above the instrument is $\leq 1 \text{ g/cm}^2$.) If a single pi-meson with an energy $E_\pi \geq 1.5 \times 10^9 \text{ ev}$ were accompanied by mu-mesons, such an event might imitate an electron in the SEZ-12 instrument.

It is known that pions with $E_\pi \geq 10^9 \text{ ev}$ are mainly generated by protons with energies $\geq 10^{10} \text{ ev}$, that is, as a rule the generation of several charged particles will take place. For this reason it is highly probable that at least one particle of any shower will strike the shower detector (8).

b. Operating Principles of the SEZ-12

Pulses from the PEM-1 photomultiplier are fed into a differential amplitude discriminator which isolates the particles having a charge $Z = 1$. (The "window" of this discriminator takes in 90 percent of the particles with $Z = 1$ passing through the solid angle of the instrument.) The pulses from the discriminator are fed into binary and ternary coincidence circuits. Pulses from the PEM-2 photomultiplier are also input, after shaping, into binary and ternary coincidence circuits.

Pulses from the PEM-3 photomultiplier are fed into a ternary coincidence circuit after shaping. /29

The binary and ternary coincidence circuits emit the "elementary" signals S_2 and S_3 .

The S_2 signal indicates a singly-charged particle passing through the telescope (i.e., passing through the solid angle of the instrument).

The S_3 signal indicates a singly-charged particle passing through the solid angle of the instrument and generating Cerenkov radiation in the gas-filled Cerenkov counter, i.e., a particle with a Lorenz factor $\gamma \geq 10$.

Pulses from the PEM-4 photomultiplier (the energy detector) actuate the integral discriminators producing the elementary signals E_i ($i = 1$ to 6).

If the amplitude of PEM-4 pulses is expressed in units of the signal most likely to be generated by a cosmic ray mu-meson passing clear through the energy detector, the thresholds expressed in these units will be equal to:

$$E_1 = 1; E_2 = 3,3; E_3 = 33; E_4 = 100; E_5 = 330; E_6 = 1000.$$

Pulses from the PEM-5 after passing through the shaper generate the elementary signal "0" ("marker").

The elementary signals S_2 , S_3 , E_i and "0" are then input to coincidence circuits, counted, and stored in the memory cells.

The various combinations of elementary signals are interpreted as follows:

1. The combination S_2 , E_i and "0" indicates that a particle with $Z = 1$ has passed through the solid angle of the SEZ-12 and released energy E_i in the energy detector, and that it (or products of its interaction) has passed through the lead filter.

2. The combination S_2 , E_i without "0" indicates the same circumstances as the foregoing, except that the particle and all secondary products /30

have been absorbed in the filter. (In a certain percentage of cases signals of this type may indicate that the secondary particles have exited through the sides of the filter.)

3. The combination $S_3 E_i$ and "0" indicates the same circumstances as 1, above, but for a particle having a Lorentz factor $\gamma \geq 10$.

4. The combination $S_3 E_i$ without "0" indicates the same circumstances as 2, above, but for a particle having a Lorentz factor $\gamma \geq 10$.

If passage of a particle through the instrument is accompanied by pulses from the PEM-6 photomultiplier (i.e., actuates the shower detector), all the events in question are automatically excluded from the recording.

3) Instrument for Studying Particles Affected by the Geomagnetic Field (SEZ-1)

The SEZ-1 instrument (energy and charge spectrometer) is designed for studying the chemical composition and energy spectrum of cosmic ray particles which are subject to the effect of the Earth's magnetic field.

A schematic diagram of the SEZ-1 is given in figure 13 (sic).

The scintillators 1 and 2 and the PEM-2 photomultiplier form counters defining the solid angle within whose limits particles are registered.

The Cerenkov counter which measures the charge of the detected particles consists of a piece of plexiglass (3) 3 cm thick and a photomultiplier (PEM-3). The upper surface of the Cerenkov detector is painted black.

The SEZ-1 instrument has a geometrical factor $\Gamma = 133 \text{ cm}^2 \text{ ster}$. The large value of Γ and the instrument's sensitivity to the direction of movement of the particles registered which make it possible in principle to take /31 advantage of the amplitude asymmetry of cosmic rays in the region of the

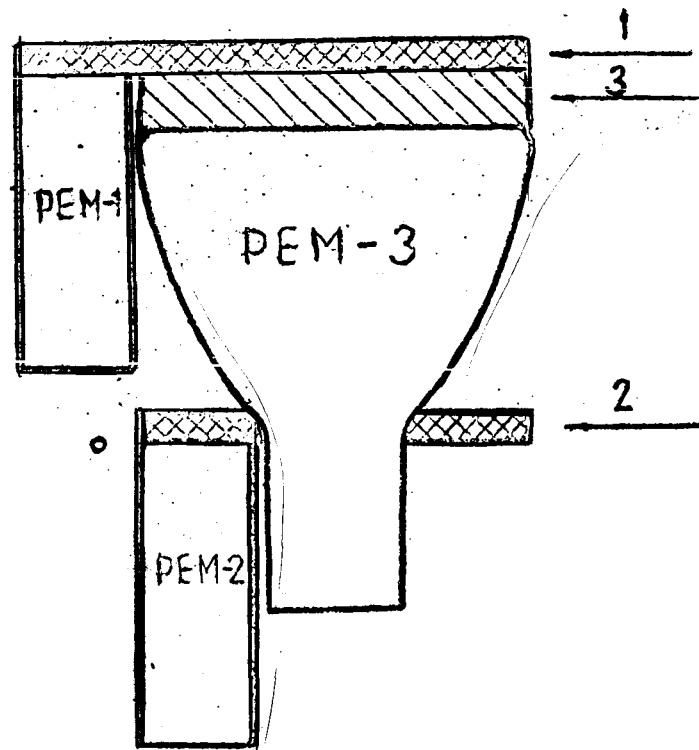


Figure 16. Schematic Diagram of SEZ-14 (sic) Instrument. 1, (with PEM-1) scintillation counter; 2, (with PEM-2) scintillation counter; 3, (with PEM-3) Cerenkov counter.

equator to make direct measurements of the energy spectrum of protons with energies up to $E_p \approx 6 \times 10^{10}$ ev and to study the chemical composition of cosmic ray particles up to energies $\sim 3 \times 10^{10}$ ev/nucleon.

In addition, the high luminosity of the instrument permits study of cosmic ray variations in various charge regions Z during long measurement series.

Pulses from the PEM-1 and PEM-2 photomultipliers are input after shaping to a binary coincidence circuit which produces the signal Z_2 .

Pulses from the PEM-3 photomultiplier activate the integral discriminators Z_i which identify particles with various charges Z .

Z_1 indicates protons.

Z_2 indicates alpha-particles and Li nuclei.

Z_3 indicates the Be, B group of nuclei.

Z_4 indicates the C, N, O group of nuclei.

Z_5 indicates the group of nuclei with $Z = 9$ to 15.

Z_6 indicates the group of nuclei with $Z = 16$ to 20.

Z_7 indicates the group of nuclei with $Z = 21$ to 30.

Z_8 indicates the group of nuclei with $Z = 31$ to 40.

Z_9 indicates the group of nuclei with $Z \geq 41$.

The instrument identifies coincidences of the type $S_2 \cap Z_i$ which are counted and stored in the memory system.

In addition, the number of binary coincidences S_2 are recorded.

4) Instrument for Recording High-Energy Gamma-Quanta (GG-1)

The GG-1 instrument is designed to record high-energy ($E_\gamma \geq 50$ Mev) gamma-quanta and to measure their energy spectrum in the energy region from $\sim 10^8$ to 3×10^9 ev.

The GG-1 is based on the instrument described by Clark and Kraushaar [32] (ref. 11). It was highly essential to repeat their experiment using similar apparatus in order to have a basis of comparison with their data involving a minimum of different and sometimes rather uncertain computational conversions.

A schematic diagram of the GG-1 instrument is given in figure 17.

The radiator in which the conversion of gamma-quanta takes place consists of a sandwich crystal scintillator made of 9 plates of scintillating plastic (1)

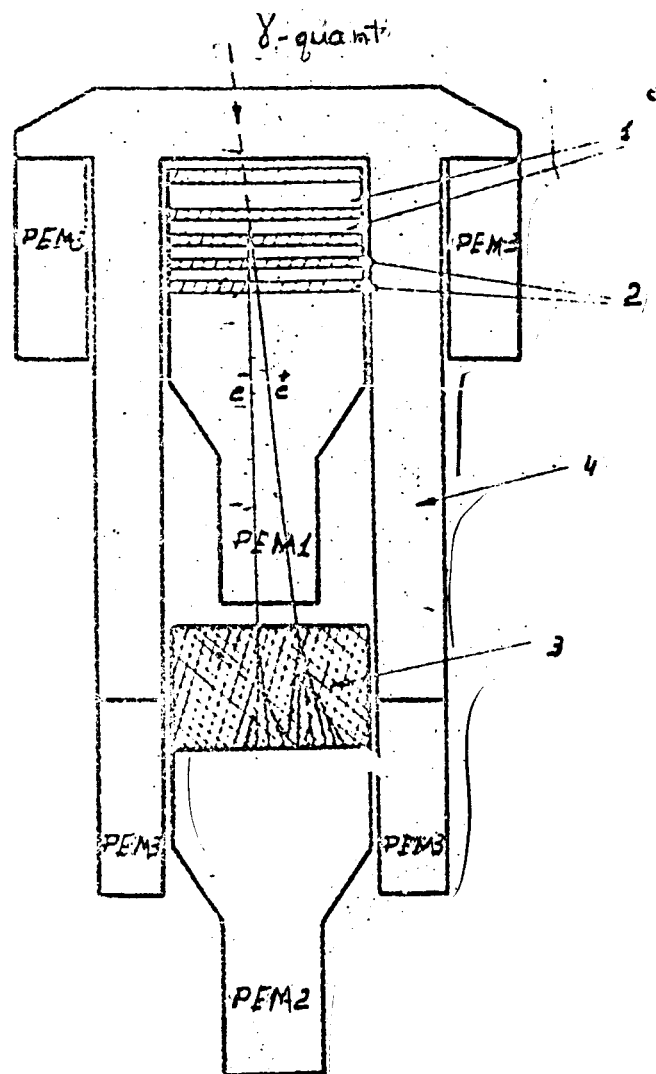


Figure 17. Schematic Diagram of GG-1 Instrument.

1, Plate of CsI (Tl); 2, scintillating plastic plate; 3, lead glass Cerenkov counter; 4, anti-coincidence scintillator shell.

each 3 mm thick and 8 plates of CsI(Tl) (2) each 2 to 2.2 mm thick. The total thickness of the radiator is about 1.1 shower units.

The sandwich crystal scintillator faces the PEM-1 photomultiplier.

Below the PEM-1 is a Cerenkov detector (3) made of lead glass 5 cm (2.5 shower units) thick. The upper surface of the Cerenkov detector is painted black, and the polished lateral surfaces are aluminized.

Light from the Cerenkov detector is registered by the photomultiplier PEM-2.

The Cerenkov detector fulfills two functions. Firstly, it registers only those particles which pass through the instrument from top to bottom (from the phosphor to the Cerenkov counter); and secondly, in the lead glass an electron-photon shower is generated and the amplitude of the light flash is approximately proportional to the energy of the primary gamma^a-quantum E_γ .

The sandwich crystal scintillator and Cerenkov counter are enclosed in an anticoincidence scintillating plastic bell (4) faced by 6 photoelectric multipliers PEM-3. /33

Appropriate electronic circuits in the instrument exclude cases of the imitation of a gamma-quantum by a slow pi-meson passing from bottom to top (within the limits of the solid angle) and stopping in the sandwich crystal, where pi-mu-electron decay yields an electron with an energy $E_\gamma \approx 50$ Mev within the solid angle of the instrument producing a pulse in the Cerenkov counter corresponding to a gamma-quantum with an energy $E \approx 50$ Mev. (Note that this type of imitation is not possible at higher energy thresholds.)

Operating Principles of the GG-1

Pulses from the Cerenkov counter (PEM-2) are input to a fast coincidence circuit with a resolution time of $\sim 5 \times 10^{-8}$ sec, which also receives a fast signal from the PEM-1 initiated by a light flash in the plastic scintillators of the phosphor. The fast coincidence circuit produces the elementary signal S_2 . (The intensity of S_2 signals is proportional to the flux of charged particles passing through the instrument within the limits of the solid angle defined by the sandwich crystal scintillator and Cerenkov detector.)

In addition, the pulse from the Cerenkov detector actuates a series of integral discriminators producing elementary signals E_i ($i = 1$ to 4). E_1 indicates the pulse most likely to be generated by the passage through the Cerenkov counter of a single relativistic particle; E_2 indicates passage of 3 particles; E_3 , of 10 particles; and E_4 , 30 particles.

The amplitudes of the fast component (from the plastic scintillators) and of the slow component (from the CsI) of the light flash generated in the sandwich scintillator are analyzed by a comparison circuit.

If these amplitudes differ by a factor not exceeding 2 to 2.5, the signal S_Y is emitted; if the difference is greater, the signal $S_n = S_2$ is /34 produced.

The elementary signals S_Y and E_1 , S_n and E_1 are then input to binary coincidence circuits connected to the counting registers of the memory, which count the number of S_Y , E_1 -type events and the number of S_n , E_1 -type events. A signal permitting recording of coincidences of these types is produced only when the binary coincidence signal S_2 is not accompanied by the passage of a charged particle through the anticoincidence shell (4).

5) Arrangement of the Scientific Apparatus on the "Proton-1" Space Station

The SEZ-1, GG-1, and SEZ-12 instruments are mounted on the SEZ-14 in such a way as to be outside the solid angle of both SEZ-14 ionization calorimeters.

This entire complex was placed in a sealed compartment on the "Proton-1" space station.

Inside this compartment, normal pressure and humidity were maintained. An automatic thermoregulating system ensured the maintenance of a temperature inside the compartment within the normal operating range of the scientific equipment.

Thickness of the compartment walls did not exceed 1 g/cm^2 within the solid angle limits of all the instruments.

In order to reduce the probability of registering secondary gamma-quanta which might be generated by interaction of primary cosmic rays with the material of the compartment walls, the GG-1 instrument was placed as close as possible to the wall. The distance between the compartment wall and the anticoincidence ^{scintillating} plastic shell (4) was not over 2 cm.

If any neutral pi-mesons generated are accompanied by even a single /35 charged particle, the probability at this short range is almost 100 percent that such a particle will strike the anticoincidence shell of the GG-1 instrument and prevent registration of the corresponding gamma-quanta.

The preceding sections of this report have stated the scientific objectives of cosmic ray study and described in detail the scientific apparatus for achieving these objectives.

Let us review this material briefly:

The SEZ-14 instrument consists of two identical parts which function independently of each other. Each part includes (fig. 4):

1. An ionization calorimeter whose ionization detectors are plastic scintillators. The ionization calorimeter measures the energy E of the primary particle.
2. An interaction detector measuring the number of particles in a shower passing through the detector.
3. Two proportional counters measuring primary particle charge.
4. Polyethylene and graphite filters which periodically exchange places or are moved outside the solid angle of the instrument during flight.

These measurements provide the material for a multidimensional amplitude analysis of the quantities E , N , and Z . Electronic equipment has independently recorded the quantities E_i , Z_j and N_k , and their combinations for various index values i , j , and k indicating the magnitude of the corresponding parameters.

Table 1 shows the measurement range of these parameters.

Table 2 gives the basic quantities measured by the SEZ-14. Those parameters which are simultaneously measured to determine the relevant physical quantity are given together in parentheses.

The SEZ-12 instrument (fig. 14) registers particles with a single electrical charge, whether or not they generate Cerenkov radiation in a gas /39

TABLE 1

/37

Particle or process parameter	Range of measurement of that parameter
Энергия первичной частицы E_i Primary particle energy	$E_1 \geq 10^{10}; E_2 \geq 3 \cdot 10^{10};$ $E_3 \geq 10^{11}; E_4 \geq 3 \cdot 10^{11};$ $E_5 \geq 10^{12}; E_6 \geq 3 \cdot 10^{12};$ $E_7 \geq 10^{13}; E_8 \geq 3 \cdot 10^{13};$ $E_9 \geq 10^{14}; \quad i = 1 \div 9.$
Primary particle charge Z_j	$Z_1 = 1; Z_2 = 2; Z_3 = 3 \div 5;$ $Z_4 = 6 \div 8; Z_5 = 9-15; Z_6 = 16 \div 20;$ $Z_7 = 21-30;$ $Z_8 = 31-40; Z_9^{40} \div j = 1 \div 9.$
No. of particles simultaneously passing through interaction detector N_K	$N_1 = 1; N_2 \geq 2; N_3 \geq 50;$ $N_4 \geq 200; N_5 \geq 500; N_6 \geq 10^3;$ $N_7 \geq 3 \cdot 10^3; \quad K = 1 \div 7.$

TABLE 2

Physical quantity being measured	Simultaneously measured parameters
Energy spectrum of all particles (independently of direction of movement or value of charge)	$E_i \quad i = 1 \div 9$
Energy spectrum of particles with a given charge	$(Z_j, E_i); j = 1 \div 9$
Protons passing through a given filter a) without interaction b) with interaction	$(Z_i, N_1, E_i); i = 1 \div 9$ $(Z_i, N_2, E_i); i = 1 \div 9$
Proton-generated ionization bursts under a compound carbon (polyethylene and lead filter)	$(Z_i, N_K); K = 3 \div 7$

and whether they are absorbed by or pass through a 12 cm lead filter. The energy of electron showers in the lead, whether generated by primary electrons or by protons of sufficiently high energy, is measured for all particles. Energies are measured in the interval from 3×10^8 ev to 2×10^{10} ev.

Particles with a Lorentz factor greater than 10, an energy greater than 3×10^8 ev, and which are absorbed in a 12 cm layer of lead, are counted as electrons.

The GG-1 instrument (fig. 17) is basically similar to that first used by Clark and Kraushaar (ref. 11), for measuring primary gamma-quantum flux. It

differs in that its Cerenkov counter is made of lead glass of 2.5 radiation units thick. This permits estimation of the energy of the registered gamma-quanta.

The SEZ-1 instrument (fig. 16) registers particles with various charges Z according to the magnitude of the pulse in the Cerenkov counter.

The "Proton-1" space station, as stated above, was launched on 16 July 1965.

So far a very small portion of the experimental material has been processed.

Preliminary results obtained from the processing of scientific information from the "Proton-1" station are given in figures 18 through 20.

Figure 18 gives the energy spectrum of primary particles as measured by 4 independently functioning instruments: the 2 ionization calorimeters (spectrum of all particles) and the 2 interaction detectors (ionization bursts generated by protons) of the SEZ-14. In addition, the proton spectrum /40 was also measured by one of the ionization calorimeters of the SEZ-12 instrument.

It is an essential feature of these measurements that the spectrum was measured over an energy range embracing 4 orders of magnitude by a single instrument, the lower limit of measured energies being below 10^{10} ev. This permitted calibration of the instrument (1st energy threshold), by the cosmic ray latitude effect.

Figure 18 shows that the experimental spectrum gives a high-energy particle intensity 10 times less than that obtained by measurement of extensive air showers (ref. 6).

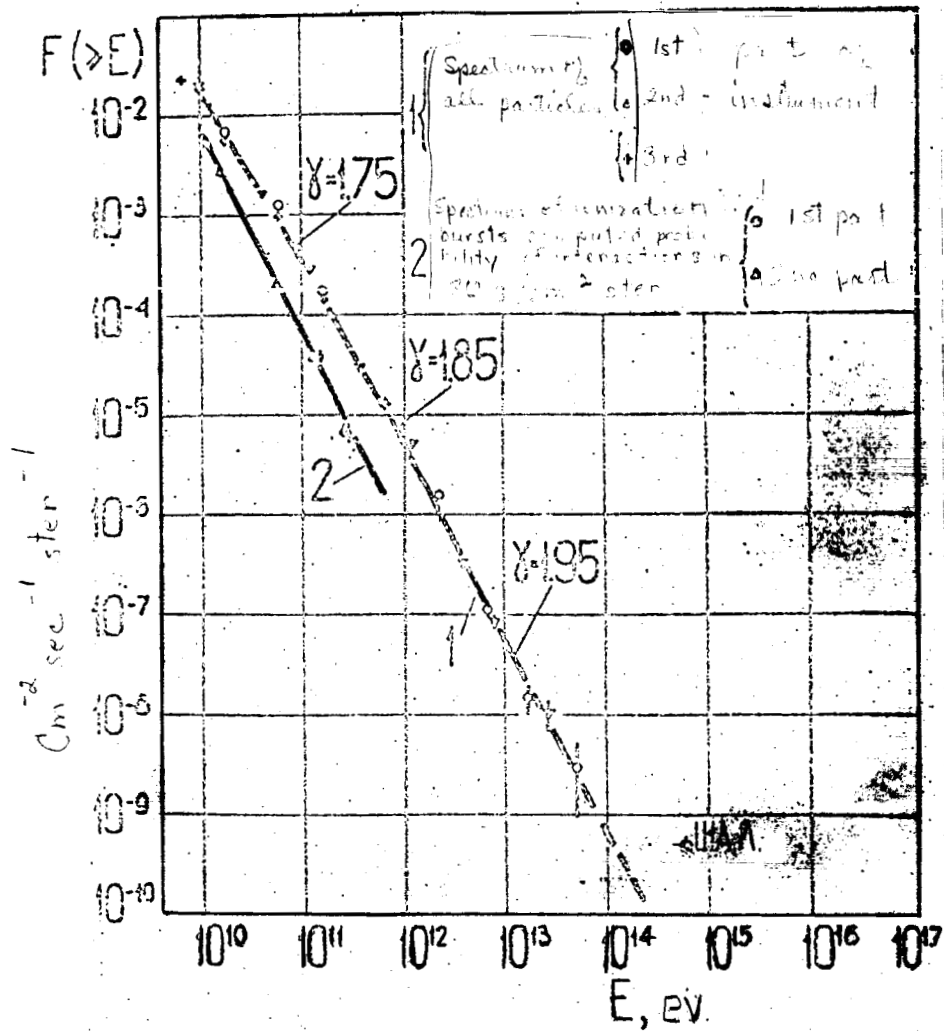


Figure 18. Energy Spectrum of Primary Cosmic Ray Particles.

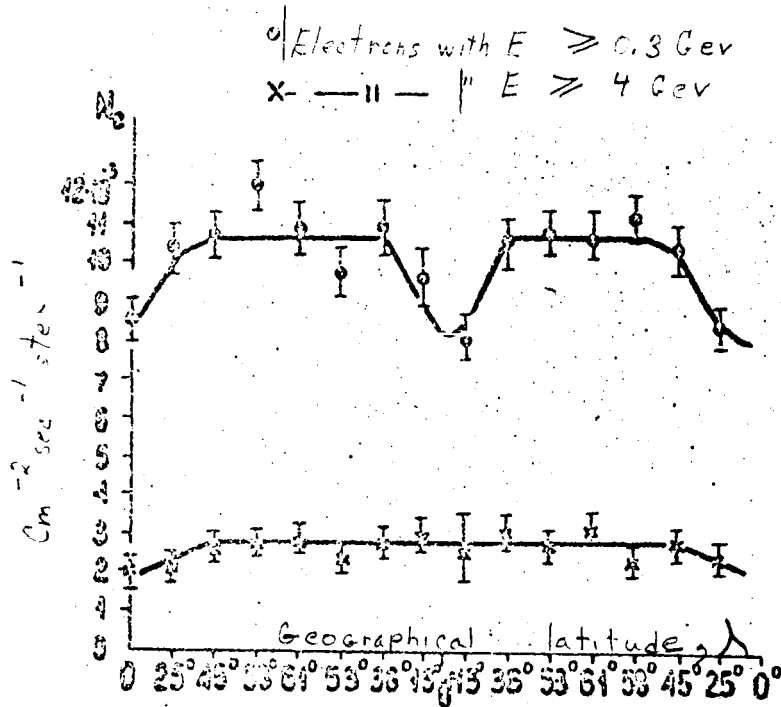


Figure 19. Dependence of Electron Intensity on Latitude λ .

In the energy region from 10^{10} to 10^{12} ev, the spectra of protons and multiply-charged particles were similar.

Figure 19 gives the results of measurement of electrons with energies greater than 0.3 and 4 GeV at various latitudes. The geographical latitudes are given on the abscissa and the electron intensity on the ordinate.

As can be seen from figure 19, beyond the atmosphere electron intensity is approximately 4 percent of 5 percent of primary proton intensity, the majority of these electrons apparently being of secondary origin.

Identification of galactic electrons requires measurements of high statistical accuracy; this will be possible once the whole body of available experimental material has been processed.

Figure 20 gives the results of measurements of the energy spectrum of gamma-quanta. These measurements were made during the initial period of the

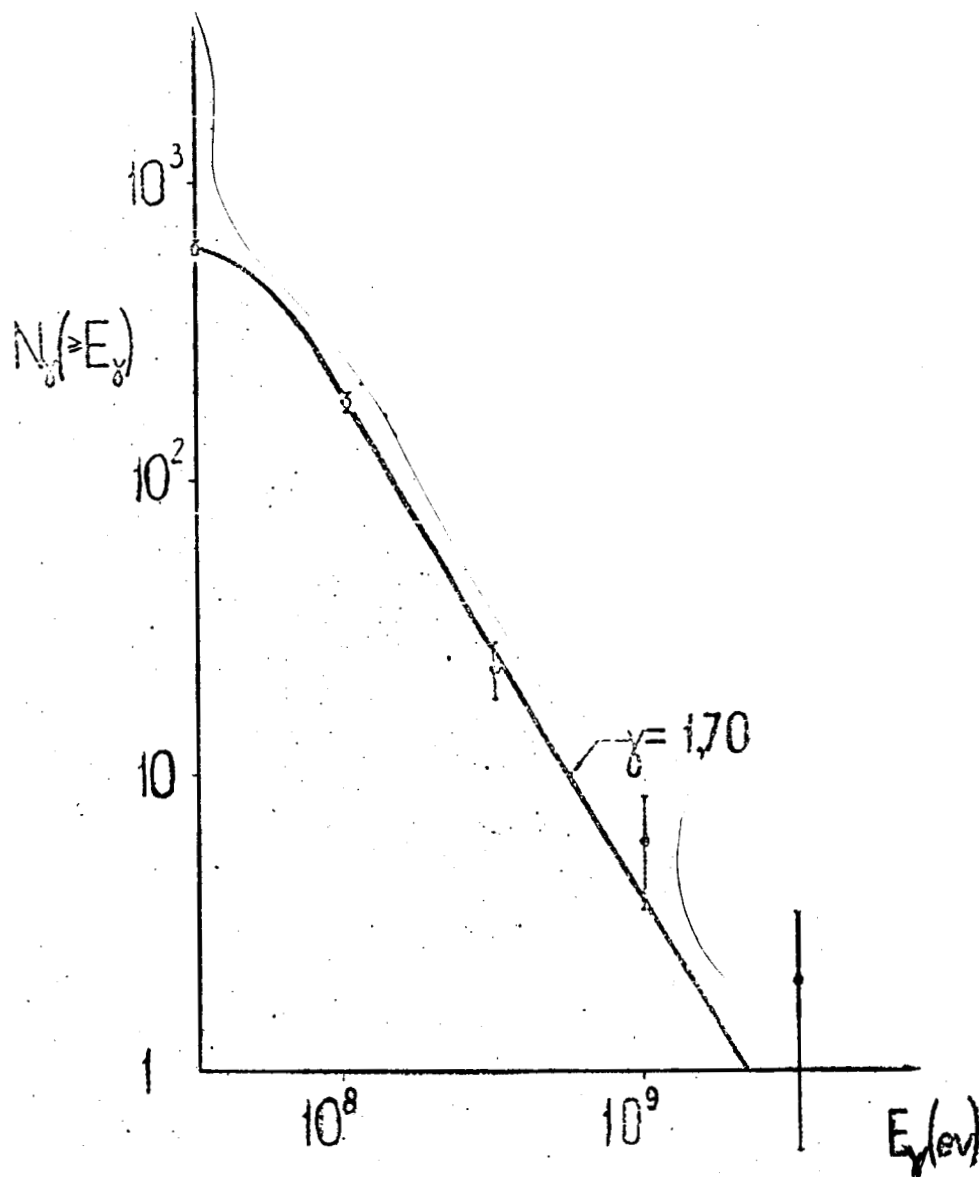


Figure 20. Energy Spectrum of Gamma-Quanta.

flight of the "Proton-1" space station, when the axis of the GG-1 instrument lay for a long time in the horizontal plane. These spectrum measurements /41 therefore refer mainly to gamma-quanta of the albedo.

Later on, when the full picture of the rotation of the "Proton-1" station has been established, it will be quite possible to obtain the energy spectrum of galactic gamma-quanta.

The following persons took active part in designing various elements, instruments, and electronic components and in the construction and installation

of the complex of primary cosmic ray study apparatus on the "Proton-1" station:

Titenkov A. F., Kalinkin L. F., Melioranskiy A. S., Pryakhin Ye. A., Volodichev N. N., Klintsov Yu. S., Savun O. I., Kovrizhnykh O. M., Smirnov A. V., Shiryayeva V. Ya., Trigubov Yu. V., Mineyev Yu. V., Shishkov P. I., Mishchenko L. G., Kakhidze G. P., Sysoyev Ye. A., Yakovlev B. M., Yurchenko Zh. D., Myratov A. S., Ben'kovskiy O. B., Nechayev O. Yu., Podrezan B. K.

REFERENCES

1. Pravda, No. 198, 17 July 1965.
2. Pravda, No. 211, 30 July 1965. /42
3. Pravda, No. 219, 7 August 1965.
4. Kaplon, M. F., Klose, I. Z., Ritson, D. M. and Walker, W. D. Physical Review, Vol. 91, 1573 (1953).
5. Baradzey, L. T., Rubtsov, V. I., Smorodin, Yu. A., Solov'yev, M. V. and Tolkachev, B. V. Trudy Fizicheskogo Instituta AN SSSR imeni P. N. Lebedeva, Vol. 26, Izd-vo Nauka, 1964.
6. Nikol'skiy, S. I. Uspekhi fizicheskikh nauk., Vol. 78, No. 3, 365, 1962.
7. Babetskiy, Ya. S., Buya, Z. A., Grigorov, N. L., Loskevich, Ye. S., Massal'skiy, Ye. I., Oleyev, A. A. and Shestoperov, V. Ya. Zhurnal eksperimental'noy i teoreticheskoy fiziki, Vol. 40, 1551, 1961.
8. Grigorov, N. L., Sobinyakov, V. A., Tret'yakova, Ch. A., Shestoperov, V. Ya., and Dulyan, Kh. P. Babayan. Report to the International Cosmic Ray Conference (Doklad na mezhdunarodnoy konferentsii po kosmicheskim lucham). London, 1965.

9. Grigorov, N. L., Rapoport, I. D., Savenko, I. A. and Skuridin, G. A.
Kosmicheskiye issledovaniya, Vol. 2, No. 5, 724, 1964.
10. Grigorov, N. L., Nesterov, V. Ye., Rapoport, I. D., Savenko, I. A. and
Skuridin, G. A. Study of High- and Superhigh-Energy Particles and the
Electron-Photon Component of Primary Cosmic Rays on the "Proton-1"
Station (Izucheniye chastits vysokikh i sverkhvysokikh energiy i elek-
tronno-fotonnoy komponenty pervichnykh kosmicheskikh luchey na stantsii
"Proton-1"). Report to the International Cosmic Ray Conference (Doklad
na mezhdunarodnoy konferentsii po kosmicheskim lucham). London, 1965.
11. Kraushaar, W. L. and Clark, G. W. Physical Review Letters, Vol. 8, 106,
1962.
12. Grigorov, N. L., Nesterov, V. Ye., Rapoport, I. D., Savenko, I. A. and
Skuridin, G. A. Report to the International Cosmic Ray Conference
(Doklad na mezhdunarodnoy konferentsii po kosmicheskim lucham). London,
1965.